GL018601

UNITED STATES DEPARTMENT OF THE INTERIOR

GEOLOGICAL SURVEY

Hydrothermal Alteration Mineralogy in Newberry 2 Drill Core, Newberry Volcano, Oregon

by

Keith E. Bargar and Terry E. C. Keith[1]

Open-File Report 84-92

[1]Menlo Park, CA

INTRODUCTION

Newberry Volcano, located in central Oregon about 40 km south of Bend, lies at the western end of a volcanic terrain that extends across much of the southeastern part of Oregon, and becomes progressively younger to the west (MacLeod and others, 1976). The caldera of Newberry Volcano contains several hot-springs, fumaroles, and young silicic obsidian flows that make this large complex volcano attractive for geothermal study (Sammel, 1981; MacLeod and Sammel, 1982). Accordingly, Newberry 2, a 932 m deep drill hole was drilled by the U.S. Geological Survey during 1978 to 1981. The hole was sited in the central part of the caldera, at an elevation of 1935 m, about 400 m east of the Big Obsidian Flow (Sammel, 1981), which is the youngest of Newberry's obsidian flows (^{14}C age of ~1300 years B.P.)(MacLeod and others, 1982)(Fig. 1).

Figure 1 near here

Sammel (1981) and MacLeod and Sammel (1982) summarize the geothermal drilling history of Newberry Volcano. According to these reports, the upper 312 m of the Newberry 2 drill hole was drilled by the mud-rotary method in 1978; the drill hole was deepened from 312 m to the hole bottom, during the summers of 1979 and 1981 by the wireline coring method. In 1981, a second offset drill hole, Newberry 3, was spudded nearby in order to obtain drill core from the upper part of the stratigraphic section from which only drill cuttings were recovered from Newberry 2. The percentage of drill core recovered from the two drill holes is reported by Sammel (1981), and MacLeod and Sammel (1982) as varying from as little as 40 percent in the upper part of the Newberry 3 drill hole to greater than 90 percent in the lower part of Newberry 2 drill hole. In order to avoid confusion, the Newberry 3 and Newberry 2 drill hole data is treated in this report as though it were obtained from a single drill hole called the "Newberry 2" drill hole.

Temperature and heat flow data for the Newberry 2 drill hole is reported in Sammel (1981), and MacLeod and Sammel (1982). The maximum temperature they recorded for the Newberry 2 drill hole is 265°C at 932 m, the hole bottom. Low temperatures of the upper part of Newberry 2 are probably due to dilution by cool meteoric water. Sammel, and MacLeod and Sammel were able to correlate some temperature changes with differences in permeability of the various rock units penetrated in the drill hole. A hypothetical conductive thermal gradient of 285°C/km for the Newberry 2 drill hole is given by MacLeod and Sammel (1982), and Sammel (1981) calculated a thermal gradient of 706°C/km for the lower 250 m of the drill hole. MacLeod and Sammel also indicate that the conductive heat flux is more than 10 times greater than the regional average value.

Newberry 2 was flow tested in late September, 1981 (Sammel, 1981). An initial wellhead pressure of 57 bars decreased to 9 bars after 20 hours of testing. Sammel (1981) and Sammel and Craig (1983) also report a gas phase

that consists predominantly of CO_2 with minor H_2S and CH_4. Unfortunately, the liquid phase recovered at this time was probably contaminated by drilling fluids (MacLeod and Sammel, 1982). Analyses of waters from nearby East Lake Hot Springs and Paulina Hot Springs are also compromised by various kinds of contamination (Mariner and others, 1975; Mariner and others, 1980) making chemical geothermometer calculations highly suspect. However, Black (1982a,b) postulates a reservoir temperature of greater than 300°C and suggests that Newberry Volcano has a significant potential for electric power generation.

The geology of Newberry Volcano and the surrounding area has been studied by several workers. Williams (1935, 1957) provided a foundation of geologic information upon which much of the later studies on such topics as airfall ash (Higgins, 1969), age relationships (Peterson and Groh, 1969; Friedman, 1977), petrography and geochemistry (Higgins and Waters, 1970; Laidley and McKay, 1971; Higgins, 1973), as well as, more recent geologic investigations (MacLeod and others, 1981; MacLeod and others, 1982) have been constructed.

HYDROTHERMAL ALTERATION

This study is primarily concerned with Newberry 2 drill core, but several pieces of Newberry 3 drill core were also studied for coverage of the interval above 312 m where only drill cuttings were obtained in the Newberry 2 drill hole. Sammel (1981) and MacLeod and Sammel (1982) furnish a preliminary generalized stratigraphic column that shows the sequence of rock units penetrated by the Newberry 2 well. Rotary cuttings of rhyolitic ash and obsidian recovered from 0-98 m were not included in this study. However, these drill cuttings are probably devoid of hydrothermal alteration as were about 40 pieces of basaltic tuff and tuff breccia core studied from 98-290 m. This interval consists mostly of unaltered glass and plagioclase crystals with minor olivine, magnetite, and clinopyroxene, although X-ray diffraction patterns do show the presence of traces of siderite at 135 m, opal(μ) at 181 m and smectite at 174 and 185 m.

Below 290 m the Newberry 2 drill hole penetrated a variety of flow units encompassing the compositional gamut of rhyodacite through dacite, andesite, basaltic andesite, and basalt, as well as fragmental rocks of about the same chemical range (Sammel, 1981; MacLeod and Sammel, 1982; Fig. 2, this report).

Figure 2 near here

Hydrothermal alteration of the several volcanic units varies from slight to pervasive with the most extreme alteration occurring along fractures and in brecciated or sedimentary zones. Several hydrothermal zeolite minerals, carbonates, clays, silica, sulfides, and minor apatite, hydrogrossular, apophyllite, gyrolite, epidote, anhydrite, and iron oxide were identified in

the volcanic sediments and lava flows encountered in the Newberry 2 drill hole between about 300 and 932 m.

ZEOLITE MINERALS

Zeolite minerals in the Newberry 2 drill core mainly are confined to two zones at 309-320 m, and 436-498 m. In the upper zone, analcime, chabazite, erionite, and faujasite were identified as vein fillings and altered glass of the basaltic sediments. The lower zone contains analcime, clinoptilolite, dachiardite, and mordenite as alteration products of glass in the rhyolitic tuff and tuff breccia. A few scattered occurrences of mordenite persist to about 748 m.

Analcime

Analcime was found at two locations in the Newberry 2 drill core. In the upper zone (313-320 m), euhedral trapezohedral analcime crystals (Fig. 3)

Figure 3 near here

occur as open space deposits in coarse basaltic sediment along with calcite, smectite, gyrolite, apophyllite, and other zeolite minerals: faujasite, chabazite, and erionite. A trace of analcime was also detected by X-ray diffraction at 444 m in association with smectite and clinoptilolite. In the upper zone the temperature measured during drilling was about 40°-50°C and in the lower zone the measured temperature was a little less than 100°C. These low temperatures are not unreasonable for the formation of analcime which appears to be somewhat independent of temperature constraints; analcime has been found over a wide temperature range (70°-300°C) in several geothermal drill holes (Kristmannsdottir and Tomasson, 1978; Honda and Muffler, 1970; Keith and others, 1978b). Instead, analcime formation appears to be favored by increasing the pH and Na^+ concentration of the associated solution (Kusakabe and others (1981).

Qualitative chemical analysis of one sample from 315 m using a Cambridge Stereoscan 180 scanning electron microscope (SEM) equipped with energy-dispersive X-ray analysis (EDAX) shows the presence of silicon, aluminum, and sodium. Two samples from 315 m and 319 m did not have a doublet d(400) X-ray diffraction peak at 3.41 Å when run at 1/4°/min. which precludes the presence of a wairakite (calcium-rich) component (Coombs, 1955). Many analcime crystals were observed by SEM to be smaller than about 10 μ in diameter (Fig. 4), and no analcime crystals were located in polished mounts

Figure 4 near here

prepared for electron microprobe studies. This may be due to the small grain size or possibly because of masking by the abundant smectite. However, the X-ray diffraction and SEM data suggest that Newbery 2 drill core analcime probably contains little, if any calcium and potassium and is probably nearly pure analcime.

Chabazite

Chabazite was identified by X-ray diffraction analysis of clear to white vein fillings and open space deposits between 309-319 m in porous basaltic sediments. Associated minerals include faujasite, chlorite, calcite, analcime, gyrolite, smectite, erionite, and apophyllite. SEM micrographs of a sample from 309 m shows that the Newberry rhombic chabazite crystals have a tabular habit and display varying degrees of flaking (desiccation ?) (Figures 5a and b) rather than the typical cube-like rhombohedra (Mumpton

Figures 5a and b near here

and Ormsby (1976). If the flaking of the crystals seen in Figures 5a and b are, in fact, due to dehydration, such effects would appear to occur at significantly lower temperatures (<50°C) than was observed for water-loss in DTA studies by Passaglia (1970) for the three chabazite chemical types he studied (sodium-rich; calcium, strontium, and potassium-rich; or calcium-rich). No chemical analyses were obtained for Newberry chabazite, but qualitative analyses by EDAX showed the presence of some sodium and potassium in addition to aluminum and silicon.

Clinoptilolite

Fibrous(?) to bladed clinoptilolite (Fig. 6) was identified by X-ray

Figure 6 near here

diffraction in six samples from 436-444 m together with smectite, siderite, calcite, and analcime. All six samples were heated overnight to 450°C in order to distinguish between clinoptilolite and heulandite by the X-ray method of Mumpton (1960). No change in intensity or position of the d(020) X-ray peak at ~9.0Å was seen, therefore, the mineral was identified as clinoptilolite. A qualitative chemical analysis of clinoptilolite from 442 m by SEM energy-dispersive X-ray analysis showed the presence of some calcium and iron in addition to sodium, potassium, aluminum, and silicon.

The clinoptilolite probably forms as an alteration product of pumiceous fragments in the rhyolitic tuff breccia. Although the X-ray diffraction

patterns clearly show the presence of clinoptilolite, some fibrous mordenite may be present in the samples studied by SEM (Fig. 6). Mordenite does occur immediately below the clinoptilolite zone and mordenite has been found to be a common companion of clinoptilolite in low temperature hydrothermal experiments starting with rhyolitic glass (Hawkins and others, 1978).

Dachiardite

Dachiardite is a fairly rare zeolite mineral that has been reported from just a few locations in the world, in basalt and andesite cavities, a silicocarbonatite sill, and hydrothermally altered rocks (Alberti, 1975; Sheridan and Maisano, 1976; Wise and Tschernich, 1978; Keith and others, 1978a; Bonardi and others, 1981; Bargar and others, 1981; Bargar and Beeson, 1981; in press). A single sample of rhyolitic tuff from 443 m in the Newberry 2 drill core contains clusters of dachiardite crystals that appear to have been formed along with smectite from altered pumice fragments.

The Newberry 2 dachiardite was deposited as a chaotic arrangement of individual acicular to ribbon-shaped crystals (Fig. 7) rather than the bundles

Figure 7 near here

of parallel crystals or polysynthetic twinned crystals usually described (Alberti, 1975; Wise and Tschernich, 1978; Bonardi and others, 1981; Bargar and Beeson, in press). Bonardi's (1979) analysis of the originally described dachiardite indicated that calcium was the more abundant cation as is the case of the Yellowstone dachiardite (Bargar and Beeson, 1981; in press). A qualitative chemical analysis of the dachiardite from Newberry Volcano suggests that the dominant cation is sodium with smaller amounts of potassium and calcium similar to sodium-rich dachiardite reported by Wise and Tschernich and Bonardi and others.

Erionite

Tiny acicular bundles of erionite crystals (Fig. 8) appear to have formed

Figure 8 near here

as a result of alteration of glass in three samples of basaltic sediments between about 315-319 m where the temperature measured during drilling was ~50°C. Minerals associated with the erionite occurrence include smectite, analcime, chabazite, faujasite, calcite, apophyllite, and gyrolite. A qualitative chemical analysis of the erionite, by EDAX, shows the presence of magnesium, calcium, iron, potassium, sodium, aluminum, and silicon.

Erionite is a fairly common mineral in some altered sedimentary tuffs and has been found as cavity fillings in mafic rocks (Gude and Sheppard, 1981). However, erionite previously has been identified in only a few hydrothermally altered rocks from geothermal drill holes in Yellowstone National Park (Honda and Muffler, 1970; Keith and Muffler, 1978; Keith and others, 1978; Bargar and Beeson, 1981). In all of the Yellowstone drill holes that contained erionite, the mineral was found near the surface where the temperatures measured during drilling were less than 110°C. The formation of erionite in sedimentary deposits and low temperature hydrothermal environments of Yellowstone National Park and Newberry Volcano suggests that the occurrence of erionite may be restricted by temperature as indicated by Honda and Muffler (1970).

Faujasite

Faujasite, a rare zeolite mineral, was identified from fracture and pore space fillings in eleven samples of basaltic sandstones between 309-320 m; associated minerals include calcite, smectite, apophyllite, erionite, gyrolite, analcime, chabazite, and hydrogrossular. The clear, intergrown, twinned (spinel law) octahedral crystals appear to be a late deposit and were observed on top of chabazite (Fig. 9) and calcite in one sample from 309 m.

Figure 9 near here

Chemical analyses were not obtained for the Newberry faujasite, but qualitative analyses by EDAX show the presence of potassium, calcium, and sodium, in addition to aluminum and silica. No magnesium was observed and the Newberry faujasite appears to be chemically more similar to that formed in Hawaiian palagonitic tuff (Iijima and Harada, 1969) rather than other occurrences in basaltic rocks of Germany (Rinaldi and others, 1975) or southeastern California (Wise, 1982). The Newberry 2 deposit is the first reported occurrence of faujasite from a geothermal system.

Mordenite

Mordenite, the most abundant zeolite mineral in the Newberry 2 drill core, occurs from 444-460 m, 469-496 m, and in three widely scattered samples between 712-748 m. Above 500 m, mordenite is confined to rhyolitic tuffs and at the top and bottom of a rhyodacite sill where it was produced by alteration of glass. Associated minerals include smectite, siderite, pyrite, calcite, chlorite, analcime, clinoptilolite and marcasite. In the lower zone, fibrous mordenite was deposited in open spaces in andesitic rocks (Fig. 10).

Figure 10 near here

Other minerals identified in the three mordenite samples from this zone include pyrrhotite, chalcedony, quartz, siderite, calcite, chlorite, and smectite. The only chemical analysis of mordenite from this drill core is a qualitative analysis by EDAX which shows just potassium, calcium, aluminum, and silicon.

APOPHYLLITE

A single sample of basaltic sandstone from ~319 m contains apophyllite in association with analcime, calcite, gyrolite, erionite, chabazite, faujasite, and smectite. The identification of apophyllite is based on a single X-ray diffraction pattern which compares well with JCPDS card 19-82. No other information is available for the Newberry 2 apophyllite since attempts to study the mineral by SEM and microprobe were unsuccessful. To the best of our knowledge, apophyllite previously has not been reported from a geothermal system; however, the mineral is not rare and is frequently associated with zeolite minerals in basalts (Dunn and others, 1978).

GYROLITE

Clusters of lamellar gyrolite crystals (Fig. 11) line a fracture at 315 m and fill pore spaces in the basaltic sandstone at 319 m along with calcite, smectite, erionite, hydrogrossular, analcime, chabazite, and faujasite. A qualitative chemical analysis of gyrolite from 319 m by EDAX only showed the presence of calcium and silicon. Gyrolite has previously been reported from a few geothermal drill holes in Iceland (Kristmannsdottir and Tomasson, 1978) and Yellowstone National Park (Bargar and others, 1981) where the temperature was considerably higher than the <50°C measured temperature for Newberry 2 gyrolite.

Figure 11 near here

CARBONATE MINERALS

Aragonite

Two samples of basaltic sandstone from about 305 m contain clear to white radiating sprays of acicular aragonite crystals that were deposited on fracture surfaces in association with calcite. This metastable calcium carbonate polymorph is commonly found in basalt amygdales. However, its presence in geothermal areas previously has been restricted to deposits on discharge pipes and channels (Browne, 1978). Microprobe chemical analyses of aragonite from 305 m (Appendix 1 and Fig. 12) shows that the mineral is

Figure 12 near here

composed of nearly pure $CaCO_3$ and very little else.

Calcite

Calcite occurs in several zones in the Newberry 2 drill core. In the upper zone, 303-321 m, calcite was identified on X-ray diffraction traces of whole-rock, fracture, and cavity-filling samples. A few of the basaltic sediment samples near the base of this zone contain nodular concretions that consist of calcite concentrations. More typically, calcite was found as thin white fracture fillings. One fracture filling from 304.5 m is composed of needle-shaped crystals (Fig. 13). Minerals associated with calcite in this

Figure 13 near here

zone are: chlorite, chabazite, faujasite, analcime, gyrolite, erionite, smectite, siderite, apophyllite, and aragonite. In the upper zone, the calcite is nearly pure $CaCO_3$ and the mineral only contains minor magnesium, iron, and manganese (Fig. 12 and Appendix 2), as well as, traces of barium and strontium.

A second zone from 435-460 m contains white massive calcite intergrown with or deposited later than siderite on fractures in altered rhyolitic pumiceous sediment. Minerals associated with the two carbonates include smectite, clinoptilolite, mordenite, pyrite, marcasite, and chlorite. Calcite from this zone contains up to about 10 weight percent $FeCO_3$+ $MnCO_3$ and less than 3 weight percent $MgCO_3$ (Fig. 12, and Appendix 2).

Calcite is notably absent from the rhyodacite sill at 460-470 m, but this carbonate mineral is prevalent again below the sill from 472-486 m in pumiceous rhyolitic sediment. Calcite was found as fracture fillings and was present in X-ray diffraction patterns of several whole rock samples. Associated minerals are siderite, smectite, chlorite, pyrite, and mordenite.

Between 486-705 m in the Newberry 2 drill core, only two samples were found that contain calcite. Fractures at 593.9 m and 595.6 m are lined by vapor-phase crystals and later white, bladed or colloform deposits of calcite along with later siderite. Below 705 m calcite is quite abundant as bladed or rhombic blocky crystals lining fractures (Fig. 14) or vesicles and as a

Figure 14 near here

replacement mineral in plagioclase phenocrysts. Minerals associated with calcite in this lower zone include most of the minerals shown in the mineral

distribution chart of Fig. 2. Calcite composition in the bottom zone can range up to about 27 weight percent $MnCO_3$+ $FeCO_3$ and only about 3 weight percent $MgCO_3$ (Fig. 12 and Appendix 2).

Ankerite-Dolomite

A few scattered samples at 335 m, 415-422 m, 690-694 m, and 739 m contain white to clear, blocky (Fig. 15a) to nearly bladed or disc-shaped

Figure 15a near here

(Fig. 15b) ankerite-dolomite crystals that were deposited in open-spaces

Figure 15b near here

between rhyodacitic and dacitic breccia fragments along with siderite, smectite, pyrite, and magnesite in samples above 700 m. Ankerite-dolomite also is deposited on bladed calcite crystals that line fracture surfaces in andesite at 739 m in association with earlier chlorite, smectite, pyrrhotite, pyrite, chalcedony, and quartz. Chemical composition of three analyzed samples indicate that the dolomite-ankerite crystals are inhomogeneous and range from ferroan dolomite to ankerite (Fig. 12 and Appendix 3). Ankerite is defined according to Deer and others (1966) as having a Mg:Fe ratio of <4:1. Most of the analyses tend to be slightly calcium-rich; however, three of the probe analyses contain much more magnesium than calcium and plot outside the dolomite-ankerite field in Fig. 12.

The temperature range for Newberry 2 ankerite-dolomite is ~80°-120°C. Dolomite from drill core Y-4 in Yellowstone Park was found at a temperature of 190°C (T.E.C. Keith, unpublished data, 1983).

Magnesite

Magnesite was identified on X-ray diffraction patterns [d(104) X-ray peak is ~2.73-2.76Å] of a few scattered rhyolitic samples from 349-365 m and between 409-422 m. Associated minerals include siderite, smectite, and ankerite-dolomite. The magnesite is not a pure magnesium carbonate, and the mineral contains significant calcium and iron (Fig. 12 and Appendix 4) in addition to minor manganese, barium and strontium. To the best of our knowledge, this is the first reported occurrence of magnesite from a geothermal system.

Siderite

Pale yellow to dark reddish-orange siderite is the dominant hydrothermal mineral between 346-715 m in Newberry 2 drill core. Siderite crystals line fractures and vesicles and fill void spaces between volcanic breccia fragments to cement the fragments. The siderite typically occurs as randomly oriented disc-shaped aggregates of rhombic crystals (Fig. 16a); occassionally

Figure 16a near here

the disc-shaped crystal clusters are found in non-random spherical or hemispherical groupings (Fig. 16b).

Figure 16b near here

Siderite from the Newberry 2 drill core is usually associated with smectite and pyrite. The paragenesis of these deposits appears to be quite variable although siderite or smectite is usually deposited earlier than pyrite. Other minerals found in the same samples as siderite include aragonite, calcite, magnesite, ankerite-dolomite, clinoptilolite, mordenite, chlorite, pyrrhotite, marcasite, quartz, opal, chalcedony, β-cristobalite, and hematite.

Hydrothermal siderite previously has been reported from geothermal drill holes in New Zealand (Browne and Ellis, 1970; Steiner, 1977) and from drill holes Y-2, Y-4, and Y-6 in Yellowstone National Park (Bargar and Beeson, 1981, in press; T.E.C. Keith, unpublished data, 19). At Broadlands, New Zealand the temperature range over which siderite was identified was 37°-130°C, and in the Yellowstone drill holes, the measured temperature varied from ~80°-180°C. Newberry 2 siderite occurs at temperatures, measured during drilling, that range from ~60°-130°C.

The above temperature brackets cannot be labeled definitely as depositional temperatures for hydrothermal siderite. However, experimental work on the formation of siderite at such low temperatures was not located in the literature and the areas listed above provide the best information we are aware of on the formation of low temperature siderite. If this temperature range should prove to be valid, then Newberry 2 siderite probably formed at temperatures not significantly different from the present-day temperature.

Newberry 2 siderite displays a great range of color, and varies from almost clear to very pale yellow, orange, caramel, and dark reddish-orange. There is also some variation in the d(104) X-ray diffraction peak which ranges from 2.79Å, same as synthetic siderite given in Joint Committee for Powder Diffraction Standards (Berry and others, 1974), to 2.83Å. No correlation

between color and X-ray data was noted. This lack of correlation probably is due to great inhomogenity in chemical composition of individual crystals or crystal clusters (Fig. 12 and Appendix 5). One sample of a spherical cluster of siderite crystals (similar to those shown in Figure 16b) from 590 m has a dark nearly opaque core and is surrounded by concentric rings when viewed in cross-section. Two scans, ~90° apart, from core to rim across a slabbed surface of a spherical crystal cluster were made with the electron microprobe. The results show that the core is manganese- and calcium-rich (nearly a calcium-rhodochrosite) and iron- and magnesium-poor (Fig. 17, and

Figure 17 near here

Appendix 6). The manganese and calcium content decreases toward the rim and magnesium and iron increase outward and are most concentrated in the rim.

APATITE

Hexagonal, tabular apatite crystals line a cavity at 910 m in the Newberry 2 drill core where the temperature measured during drilling was about 250°C. Associated minerals include calcite, quartz, pyrite, and later chlorite (Fig. 18). Hydrothermal apatite previously has been identified as an open space

Figure 18 near here

deposit in drill core Y-6 from Yellowstone National Park at a temperature of about 100°C (Bargar and Beeson, in press) and as pseudomorphs after hornblende and hypersthene in drill holes in the Wairakei Geothermal Area, New Zealand (Steiner, 1977). Apatite also occurs as a minor constituent in a few other geothermal areas such as Steamboat Springs, Nevada (Sigvaldson and White, 1961), Milos, Greece (Fytikas and others, 1976), Cesano, Italy (Funiciello and others, 1979), and Larderello, Italy (Cavarretta and others, 1980).

HYDROGROSSULAR

A whole rock X-ray diffraction diagram of basaltic sediment (?) from about 315 m in the Newberry 2 drill core showed that the sample consists almost completely of hydrogrossular crystals (Fig. 19). The nearly isotropic

Figure 19 near here

reddish crystals appear to be trapezohedral in scanning electron micrographs (Fig. 20). A qualitative chemical analysis by EDAX shows the presence of

Figure 20 near here

calcium, aluminum, iron, and silicon; the four most abundant elements of some hydrogrossular analyses (Gross, 1977). A second piece of core from the same depth contained no garnet, but the sample has abundant analcime and traces of calcite, gyrolite, chabazite, and faujasite.

Garnet has been identified previously in the Iceland and Salton Sea geothermal areas (Browne, 1978). The origin of the Iceland garnet has been attributed to contact metamorphism (Kristmannsdottir, 1981; Mehegan and others, 1982); whereas, the Salton Sea garnet is believed to be hydrothermal (Freckman, 1978).

CLAY MINERALS

Smectite

Smectite is the pincipal clay mineral in the Newberry 2 drill core between ~300-750 m. Buff to dark green smectite occurs primarily as a fracture filling intergrown with siderite and pyrite throughout much of the interval. Smectite is also found as vesicle fillings and in the matrix of several highly altered samples of drill core. Nearly every mineral found in the Newberry 2 drill core is associated with smectite. Smectite is noticeably absent from the rhyodacite flow at ~500-550 m.

Detailed X-ray diffraction studies of smectite in this drill core show d(001) basal spacings that range from ~12.6-16.1 Å; the basal spacing expands to ~16.4-18.3 Å after glycollation at 60°C for 1 hour. In the lower part of the smectite interval shown in Fig. 2 (below about 700 m), the clay mineral consistently expands to less than 17 Å after being glycollated, and the clay may consist of randomly interstratified chlorite-smectite (P. Hauff, written communication, 1982) with smectite being the predominant mineral. However, these clay deposits are plotted along with smectite in Fig. 2.

Variability in the unglycollated d(001) spacing suggests some variation in the exchangeable cation (Grim, 1968). Qualitative chemical analysis by EDAX of several samples shows the presence of silicon, aluminum, and iron in all the samples analyzed. Elements also present in one or more of the analyzed samples are potassium, calcium, sodium, magnesium, and titanium. The refractive index of one sample was 1.58-1.59 suggesting that the smectite species is nontronite. Crystal habit varies from irregular sheet structure to stacks of platey crystals (Fig. 21). The irregular sheet-like morphology was

Figure 21 near here

also observed in a spherical cluster of smectite crystals (Fig. 22).

Figure 22 near here

Illite-Smectite

White interstratified illite-smectite was identified in a narrow very altered breccia zone at 793.5-795 m below the surface of the drill hole. The mixed-layer clay is associated with calcite, chlorite, smectite, pyrite, and quartz, and appears to be an alteration product of phenocryst plagioclase.

X-ray diffraction data for the two samples show a $(00\ell)_I/(00\ell)_S$ spacing of about 10.7Å that contracts to about 9.7Å (smectite peak not seen) after being glycollated at 60°C for 1 hour. These two samples appear to be a randomly interstratified illite-smectite (Hower, 1981). A third sample has an 11.4Å peak and a 9.0Å peak after being glycollated. This sample is probably an "allevardite" ordered interstratified illite-smectite (Hower, 1981). The percentage of illite layers in all three samples appears to be ~60 percent or greater.

Illite

Green illite (refractive index ~1.55-1.56), intergrown with chlorite (Fig. 23), occurs at 752-761 m, 772 m, 908-909 m, and 930-932 m in the

Figure 23 near here

Newberry 2 drill core. This clay mineral is mostly confined to breccia zones. In addition to chlorite, associated minerals include calcite, pyrrhotite, pyrite, quartz, and smectite. A qualitative chemical analysis by EDAX shows the presence of potassium, iron, aluminum, and silicon.

Chlorite-Smectite

Scattered samples, below 742 m in the drill core, contain green, mixed-layer chlorite-smectite or corrensite. The ordered interstratified clay mineral is associated with chlorite, smectite, pyrrhotite, pyrite, chalcedony, quartz, illite, hematite, apatite, and anhydrite. Chlorite-smectite is found

as a lining on fractures and in vesicles and is present in a few altered whole rock samples replacing interstital glass in andesites and basalts. Figures 24 and 25 show the sheet-like morphology of the mixed-layer clay mineral, as well

Figures 24 and 25 near here

as the rosette habit of clusters of the platey crystals.

X-ray diffraction traces of ordered interstratified chlorite-smectite from the Newberry 2 drill core contain higher order 28-29Å X-ray peaks in addition to 14Å and 7Å peaks that exhibit a slight expansion when glycollated (Hower, 1981). From the X-ray data, it appears that this clay mineral contains varying proportions of chlorite and smectite without any discernable pattern throughout its distribution range. Identification of the mineral is often made difficult because of the presence of other clay minerals on X-ray diffraction patterns. Qualitative chemical analyses by EDAX shows that two samples of chlorite-smectite from Newberry 2 drill core consist mostly of iron, magnesium, calcium, aluminum, and silicon.

Swelling chlorite and randomly mixed-layer chlorite-smectite have been described in Iceland's Reykjanes geothermal area at temperatures of 200°-270°C (Kristmannsdottir, 1976). In the Newberry 2 drill core, there appears to be a progression of smectite to random interstratified chlorite-smectite to ordered interstratified chlorite-smectite to chlorite over the present temperature range of about 150°-265°C (Fig. 2). This temperature range more than encompasses the Iceland temperature range, and both temperature ranges are considerably higher than the pre-greenschist facies metamorphic temperatures (~100°-150°C) for the formation of corrensite in sandstones and volcanogenic rocks (Hoffman and Hower, 1979). Newberry 2 temperatures may have been even higher in the past than the measured temperatures indicate because fluid inclusion homogenization temperatures in quartz crystals (discussed below) show temperatures that exceed the measured temperature over the same depth range. However, the clay minerals were usually deposited later than quartz and the actual formational temperatures for the clays is perhaps somewhere between the fluid inclusion temperatures and the measured temperatures.

Chlorite

Chlorite was detected by X-ray diffraction at 309 m, 449-477 m, and below 707 m. In the upper occurrence, chlorite is associated with calcite, chabazite, and faujasite. The intermediate depth zone also contains siderite, calcite, mordenite, smectite, pyrite, and marcasite; and in the lower zone, chlorite was found in association with siderite, calcite, smectite, chlorite-smectite, pyrrhotite, pyrite, chalcedony, quartz, mordenite, illite, illite-smectite, hematite, and epidote. Chlorite in Newberry 2 drill core is primarily an open-space deposit on fractures and in vesicles consisting of rosettes of radiating sheet-like crystals (Fig. 26) or books of euhedral

Figure 26 near here

hexagonal platelets (Fig. 27). A qualitative chemical analysis by EDAX shows

Figure 27 near here

the presence of iron, magnesium, aluminum, and silicon.

SILICA MINERALS

Opal and β-Cristobalite

A few scattered samples between 569-642 m have fractures that are lined by clear to white powdery or colloform or orange massive amorphous silica or opal (refractive index = ~1.46). Associated minerals are calcite, smectite, pyrite, marcasite, and chalcedony. Between 700-725 m there are four samples of weakly birefringent, colorless or white, colloform β-cristobalite (refractive index = ~1.47) that were deposited on fractures. The fractures also contain smectite, pyrrhotite, pyrite, chalcedony, siderite, calcite, and quartz.

Chalcedony

Clear, white, or bluish-gray chalcedony (refractive index = ~1.53, microfibrous habit, weak birefringence) lines vesicles and coats fractures in the drill core from 556-563 m, 701-744 m, and at scattered locations between 811 and 900 m. The open-space cryptocrystalline silica deposits frequently have a colloform texture and are associated with β-cristobalite or later quartz crystals. Other hydrothermal minerals found in association with chalcedony include: siderite, smectite, pyrite, pyrrhotite, calcite, mordenite, chlorite, chlorite-smectite, and hematite.

Quartz

Clear, tiny (up to about 7 mm long), euhedral quartz crystals were deposited in vesicles and fractures between 461-469 m and below 713 m in the Newberry 2 drill core. A few samples show more than one generation of quartz crystals. The general paragenetic sequence consists of green clay (chlorite or chlorite-smectite), ± bluish botryoidal chalcedony, crystalline quartz, bladed or blocky calcite, and ± very minute quartz crystals coating calcite.

Other minerals associated with quartz include siderite, smectite, pyrite, pyrrhotite, iron oxide, marcasite, cristobalite, mordenite, dolomite-ankerite, illite, illite-smectite, epidote, anhydrite, and apatite.

Six quartz samples from various depths below 750 m were polished on two sides for fluid inclusion studies. Most of the fluid inclusions appear to be secondary; however, a few primary fluid inclusions may be included in the study. Salinity of the fluid inclusions, determined by the freezing method (Roedder, 1962), is near zero in the upper fluid inclusion samples and only about 1 percent NaCl equivalent in the bottom samples. Filling temperatures of the liquid-rich fluid inclusions range between ~171.0°-363.2°C (Fig. 28).

Figure 28 near here

The minimum homogenization temperature for three of the quartz samples is very close to the measured temperature curve, and only 5 out of 139 filling temperature measurements fall slightly below the measured temperature curve. The data indicate that in the past the temperature throughout the lower 200 m of the Newberry 2 drill hole was significantly warmer than the present temperatures.

SULFIDE MINERALS

Pyrrhotite

Tabular, bronze, pseudohexagonal pyrrhotite crystals (Fig. 29) line

Figure 29 near here

fractures and cavities and are disseminated in the drill core from 461-467 m. Pyrrhotite appears to be the earliest hydrothermal mineral deposited in this section of the Newberry 2 drill core, and is found in association with siderite, smectite, pyrite, marcasite, and quartz. A second zone of disseminated and open-space pyrrhotite deposition extends from 696-792 m. The pseudohexagonal pyrrhotite crystals (up to about 3 mm in length) in this zone appear to have been deposited later than quartz but earlier than other associated hydrothermal minerals that include siderite, smectite, pyrite, calcite, chlorite, β-cristobalite, chalcedony, and mordenite. Between 908 m and the drill hole bottom, at 932 m, are a few scattered samples containing tabular pyrrhotite in vugs and on fractures along with associated calcite, chlorite, pyrite, quartz, and illite. Some samples in the upper zone contain replacement pyrite and marcasite that is pseudomorphous after pyrrhotite (Fig. 30).

Figure 30 near here

Microprobe chemical analyses of 4 pyrrhotite samples from the two upper pyrrhotite zones in the Newberry 2 drill hole are listed in Appendix 7. The shallowest sample has less iron and sulfur, as well as, a lower total of chemical constituents than the deeper 3 samples. The low totals for the upper sample may suggest the presence of one or more elements that was not determined in the analysis; although this conclusion is currently speculative. Multiple analyses of different points within a sample show some inhomogeneity between the three lower pyrrhotites in Appendix 7. This variation in chemical composition can be seen in a plot of atomic percent iron versus temperature (phase diagram for the Fe-S system below 350°C) (Fig. 31)

Figure 31 near here

which indicates that the Newberry 2 pyrrhotite should be monoclinic (type 4c) (Kissin and Scott, 1982). Nine additional samples from the three pyrrhotite zones were X-rayed at 1/4°/min., and all nine X-ray diffractograms showed doublet X-ray peaks [d(202) and d(202)] of nearly equal intensity which suggests that a hexagonal component, if present, could only be of minor abundance (Arnold, 1966).

Browne and Ellis (1970) and Steiner (1977) report finding pyrrhotite in drill core from New Zealand geothermal areas at temperatures ranging from 152°-268°C. Pyrrhotite was identified in drill core from Yellowstone National Park at temperatures measured during drilling of 130°-152°C (Bargar and Beeson, 1981). In the Newberry 2 drill hole, the measured temperatures for depths at which pyrrhotite was found were about 97°C, 110°-180°C, and 250°-265°C in the upper, middle, and lower zones, respectively.

Pyrite

Except for 2 samples near 385 m, pyrite is absent in the drill core above 446 m and occurs in scattered concentrations below 829 m; however, cubic pyrite crystals are present in much of the intervening drill core. Pyrite is closely associated with siderite, smectite, and marcasite in the main sulfide zone (Fig. 2). Other minerals associated with pyrite include mordenite, chlorite, calcite, pyrrhotite, quartz, chalcedony, opal, cristobalite, dolomite-ankerite, chlorite-smectite, illite, illite-smectite, and apatite. Microprobe chemical analyses of 6 pyrite samples are listed in Appendix 8. In addition to somewhat varying abundances of iron and sulfur, most samples analyzed contained minor cobalt and no detectable nickel.

Marcasite

Scattered samples of marcasite were identified by X-ray diffraction between 453-627 m in the Newberry 2 drill core. Cavity and fracture deposits of marcasite are generally found closely associated with pyrite and pyrrhotite, but the "cockscomb" crystals (Fig. 32) may also occur in

Figure 32 near here

association with siderite, calcite, smectite, mordenite, chlorite, quartz, and opal.

Marcasite is metastable with respect to pyrite at low temperature (Craig and Scott, 1974) and is converted to pyrite at temperatures greater than 160°C in the Salton Sea geothermal system (McKibben, 1979). In drill core Y-6 from Yellowstone National Park, marcasite occurs at temperatures of about 80°-170°C (Bargar and Beeson, in press), and at Steamboat Springs, Nevada, marcasite was found in a few samples at temperatures below about 140°C (Sigvaldson and White, 1962). The temperature range for marcasite in the Newberry 2 drill core is about 74°-98°C.

Several microprobe chemical analyses of marcasite from 566 m (Appendix 9) shows that the mineral from this sample was fairly homogeneous with respect to both iron and sulfur, and contains no detectable cobalt or nickel.

EPIDOTE

Yellow-green epidote crystals (Figs. 33a and 33b) line vugs and fractures

Figures 33a and 33b near here

between 912-917 m in the drill core. The euhedral twinned epidote crystal clusters occur in association with earlier quartz and calcite and later (?) chlorite or chlorite-smectite; some core samples also have fine-grained, patchy, reddish hematite inclusions. Qualitative chemical analyses of epidote samples by EDAX show the presence of calcium, iron, aluminum, and silicon. The measured temperature at which epidote was found in the Newberry 2 drill hole was about 258°C, which is well above the 230°C minimum stability limit given for epidote that forms at low-pressure conditions characteristic of geothermal areas (Seki, 1972).

ANHYDRITE

Clear, blocky anyhdrite crystals formed on fractures at 914-916 m where the temperature measured during drilling was about 258°C. Hydrothermal minerals found in association with anhydrite from Newberry 2 drill core include quartz, smectite, calcite, hematite, and later chlorite-smectite (Fig. 34). The presence of anhydrite at depth in the Newberry drill core is

Figure 34 near here

probably due to oxidation of sulfides to produce sulfuric acid which reacts with calcite to form anhydrite.

IRON OXIDE

Hematite was identified by X-ray diffraction in a few vesicles, fractures, altered mafic minerals, and oxidized zones at 600 m, 805 m, 834-860 m, and 915-917 m in the Newberry drill core. Associated minerals include siderite, smectite, calcite, chlorite, chlorite-smectite, quartz, chalcedony, epidote, and anhydrite. Pyrite was found in only 1 of 24 samples containing hematite.

A narrow zone at 465-466 m contains oxidized crusts that coat pyrrhotite crystals. X-ray diffraction analyses show that the crusts are composed of sulfur, goethite, and lepidocrocite; in addition to pyrrhotite, pyrite, and marcasite. The samples also contain siderite, smectite, and quartz. The two iron oxide minerals and sulfur probably formed as by-products during alteration of pyrrhotite to pyrite and marcasite.

REFERENCES CITED

Alberti, A., 1975, Sodium-rich dachiardite from Alpe di Suisi, Italy: Contributions to Mineralogy and Petrology, v. 49, p. 63-66.

Arnold, R.G., 1966, Mixtures of hexagonal and monoclinic pyrrhotite and the measurement of the metal content of pyrrhotite by X-ray diffraction: American Mineralogist, v. 51, p. 1221-1227.

Bargar, K.E., and Beeson, M.H., 1981, Hydrothermal alteration in research drill hole Y-2, Lower Geyser Basin, Yellowstone National Park, Wyoming: American Mineralogist, v. 66, p. 473-490.

Bargar, K.E., and Beeson, M.H., in press, Hydrothermal alteration in research drill hole Y-6, Upper Firehole River, Yellowstone National Park, Wyoming: U.S. Geological Survey Professional Paper 1054-B.

Bargar, K.E., Beeson, M.H., and Keith, T.E.C., 1981, Zeolites in Yellowstone National Park: Mineralogical Record, v. 12, p. 29-38.

Berry, L.G., Post, B., Weissman, S., McMurdie, H.F., and McClure, W.R., (eds.), 1974, Selected powder diffraction data for minerals: Joint Committee on Powder Diffraction Standards, Philadelphia, Pennsylvania, 833p.

Black, G.L., 1982a, An estimate of geothermal potential of Newberry Volcano, Oregon: Oregon Geology, v. 44, p. 44-46.

Black, G.L., 1982b, A revision to the estimate of the geothermal potential of Newberry Volcano: Oregon Geology, v. 44, p. 57.

Bonardi, M., 1979, Composition of type dachiardite from Elba: a re-examination: Mineral Magazine, v. 43, p. 548-549.

Bonardi, M., Roberts, A.C., Sabina, A.P., and Chao, G.Y., 1981, Sodium-rich dachiardite from the Francon Quarry, Montreal Island, Quebec: Canadian Mineralogist, v. 19, p. 285-289.

Browne, P.R.L., 1978, Hydrothermal alteration in active geothermal fields: Annual Reviews in Earth and Planetary Sciences, v. 6, p. 229-250.

Browne, P.R.L., and Ellis, A.J., 1970, The Ohaki-Broadlands hydrothermal area, New Zealand: mineralogy and related geochemistry: American Journal of Science, v. 269, p. 97-131.

Cavarretta, G., Gianelli, G., and Puxeddu, M., 1980, Hydrothermal metamorphism in the Larderello Geothermal Field: Geothermics, v. 9, p. 297-314.

Coombs, D.S., 1955, X-ray observations on wairakite and non-cubic analcime: Mineral Magazine, v. 30, p. 699-708.

Craig, J.R., and Scott, S.D., 1974, Sulfide phase equilibria: in: P.H. Ribbe (ed.), Mineralogical Society of America Short Course Notes: Sulfide Mineralogy, p. CS1-CS110.

Deer, W.A., Howie, R.A., and Zussman, J., 1966, An introduction to the rock forming minerals: Longman, London, 528 p.

Dunn, P.J., Rouse, R.C., and Norberg, J.A., 1978, Hydroxyapophyllite, a new mineral, and a redefinition of the apophyllite group I. Description, occurrences, and nomenclature: American Mineralogist, v. 63, p. 196-202.

Freckman, J.T., 1978, Fluid inclusion and oxygen isotope geothermometry of rock samples from Sinclair 34 and Elmore #1 boreholes, Salton Sea Geothermal Field, Imperial Valley, California, U.S.A.: University of California, Riverside, MS thesis, 155p.

Friedman, I., 1977, Hydration dating of volcanism at Newberry Crater, Oregon: Journal of Research of the U.S. Geological Survey, v. 5, p. 337-342.

Funiciello, R., Mariotti, G., Parotto, M., Preite Martinez, M., Tecce, F., Toneatte, R., and Turi, B., 1979, Geology, mineralogy, and stable isotope geochemistry of the Cesano geothermal field (Sabatini Mtns. Volcanic system, Northern Latium, Italy): Geothermics, v. 8, p. 55-73.

Fytikas, M., Kouris, D., Marbaelli, G., and Surcin, J., 1976, Preliminary geological data from the first two productive geothermal wells drilled at the island of Milos: International Congress on thermal waters, geothermal energy and vulcanism of the Mediterranean area, Athens, Proceedings geothermal energy, v. 1, p. 511-515.

Grim, R.E., 1968, Clay mineralogy: Mcgraw-Hill Book Co., San Francisco, 596 p.

Gross, S., 1977, The mineralogy of the Hatrurim formation, Israel: Geological Survey of Israel Bulletin, No. 70, 80p.

Gude, A.J., and Sheppard, R.A., 1981, Woolly erionite from the Reese River Zeolite Deposit, Lander County, Nevada, and its relationship to other erionites: Clays and Clay Minerals, v. 29, p. 378-384.

Hawkins, D.B., Sheppard, R.A., and Gude, A.J., 3rd, 1978, Hydrothermal synthesis of clinoptilolite and comments on the assemblage phillipsite-clinoptilolite-mordenite: In L.B. Sand and F.A. Mumpton (eds.), Natural Zeolites: Occurrence, Properties, Use, Pergamon, New York, p. 337-343.

Higgins, M.W., 1969, Airfall ash and pumice lapilli deposits from central pumice cone, Newberry Caldera, Oregon: U.S. Geological Survey Professional Paper 650-D, p. D26-D32.

Higgins, M.W., 1973, Petrology of Newberry Volcano, central Oregon: Geological Society of America Bulletin, v. 84, p. 455-488.

Higgins, M.W., and Waters, A.C., 1970, A re-evaluation of basalt-obsidian relations at East Lake Fissure, Newberry Caldera, Oregon: Geological Society of America Bulletin, v. 81, p. 2835-2842.

Hoffman, J., and Hower, J., 1979, Clay mineral assemblages as low grade metamorphism geothermometers: application to the thrust faulted disturbed belt of Montana, U.S.A.: In P.A. Scholle, and P.R. Schluger (eds.), Aspects of Diagenesis. Society of Economic Paleontologists and Mineralogists Special Publication No. 26, p. 55-79.

Honda, S., and Muffler, L.J.P., 1970, Hydrothermal alteration in core from research drill hole Y-1, Upper Geyser Basin, Yellowstone National Park, Wyoming: American Mineralogist, v. 55, p. 1714-1737.

Hower, J., 1981, X-ray diffraction identification of mixed-layer clay minerals: Mineralogical Association of Canada Short Course, p. 39-59.

Iijima, A., and Harada, K., 1969, Authigenic zeolites in zeolitic palagonitic tuffs on Oahu, Hawaii: American Mineralogist, v. 54, p. 182-197.

Keith, T.E.C., and Muffler, L.J.P., 1978, Minerals produced during cooling and hydrothermal alteration of ash-flow tuff from Yellowstone drill hole Y-5: Journal of Volcanology and Geothermal Research, v. 3, p. 373-402.

Keith, T.E.C., Beeson, M.H., and White, D.E., 1978a, Hydrothermal minerals in U.S. Geological Survey research drill hole Y-13, Yellowstone National Park, Wyoming: Geological Society of America Abstracts with Programs, v. 10, p. 432-433.

Keith, T.E.C., White, D.E., and Beeson, M.H., 1978b, Hydrothermal alteration and self-sealing in Y-7 and Y-8 drill holes in northern part of Upper Geyser Basin, Yellowstone National Park, Wyoming: U.S. Geological Survey Professional Paper 1054-A, 26p.

Kissin, S.A., and Scott, S.D., 1982, Phase relations involving pyrrhotite below 350°C: Economic Geology, v. 77, p. 1739-1754.

Kristmannsdottir, H., 1976, Types of clay minerals in hydrothermally altered basaltic rocks, Reykjanes, Iceland: Jokull, 26, p. 30-39.

Kristmannsdottir, H., 1981, Wollastonite from hydrothermally altered basaltic rocks in Iceland: Mineralogical Magazine, v. 44, p. 95-99.

Kristmannsdottir, H., and Tomasson, J., 1978, Zeolite zones in geothermal areas of Iceland: In L.B. Sand and F.A. Mumpton (eds.), Natural Zeolites: Occurrence, Properties, Use, Pergamon, New York, p. 277-284.

Kusakabe, H., Minato, H., Utada, M., and Yamaneka, T., 1981, Phase relations of clinoptilolite, mordenite, analcime and albite with increasing pH, sodium ion concentration and temperature: Scientific Papers of the College of General Education, University of Tokyo, v. 31, p. 39-59.

Laidley, R.A., and McKay, D.S., 1971, Geochemical examination of obsidian from Newberry caldera, Oregon: Contributions to Mineralogy and Petrology, v. 30, p. 336-342.

McKibben, M.A., 1979, Ore minerals in the Salton Sea Geothermal system, Imperial Valley, California, U.S.A., University of California, Riverside, unpublished MS thesis, 90p.

MacLeod, N.S., and Sammel, E.A., 1982, Newberry Volcano, Oregon: A Cascade Range geothermal prospect: Oregon Geology, v. 44, p. 123-131.

MacLeod, N.S., Walker, G.W., and McKee, E.H., 1976, Geothermal significance of eastward increase of upper Cenozoic rhyolitic domes in southeast Oregon: Second United Nations Symposium on the Development and Use of Geothermal Resources, San Francisco, California, 1975, Proceedings: Washington D.C., U.S. Government Printing Office, v. 1, p. 465-474.

MacLeod, N.S., Sherrod, D.R., and Chitwood, L.A., 1982, Geologic map of Newberry Volcano, Deschutes, Klamath, and Lake Counties, Oregon: U.S. Geological Survey Open-file Report 82-847, 27p.

MacLeod, N.S., Sherrod, D.R., Chitwood, L.A., and McKee, E.H., 1981, Newberry Volcano, Oregon: In Johnston, D.A., and Donnelly-Nolan, J., (eds.), Guides to some volcanic terranes in Washington, Idaho, Oregon, and Northern California: U.S. Geological Survey Circular 838, p. 85-91.

Mariner, R.H., Presser, T.S., Rapp, J.B., and Willey, L.M., 1975, The minor and trace elements, gas, and isotopic compositions of the principal hot springs of Nevada and Oregon: U.S. Geological Survey Open-file Report, 75- , 27p.

Mariner, R.H., Swanson, J.R., Orris, G.J., Presser, T.S., and Evans, W.C., 1980, Chemical and isotopic data for water from thermal springs and wells of Oregon: U.S. Geological Survey Open-file Report 80-737, 50p.

Mehegan, J.M., Robinson, P.T., and Delaney, J.R., 1982, Secondary mineralization and hydrothermal alteration in Reydarfjordur drill core, Eastern Iceland: Journal of Geophysical Research, v. 87, p. 6511-6524.

Mumpton, F.A., 1960, Clinoptilolite redefined: American Mineralogist, v. 45, p. 351-369.

Mumpton, F.A., and Ormsby, W.C., 1976, Morphology of zeolites in sedimentary rocks by scanning electron microscopy: Clays and Clay Minerals, v. 24, p. 1-23.
Passaglia, E., 1970, The crystal chemistry of chabazites: American Mineralogist, v. 55, p. 1278-1301.
Peterson, N.V., and Groh, E.A., 1969, The ages of some Holocene volcanic eruptions in the Newberry volcano area, Oregon: The Ore Bin, v. 51, p. 73-87.
Rinaldi, R., Smith, J.V., and Jung, G., 1975, Chemistry and paragenesis of faujasite, phillipsite, and offertite from Sasbach, Kaisewrstuhl, Germany: Neues Jahrbuch fur Mineralogie, Monetahefte, p. 433-443.
Roedder, E., 1962, Studies of fluid inclusions I: Low temperature application of a dual-purpose freezing and heating stage: Economic Geology, v. 57, p. 1045-1061.
Sammel, E.A., 1981, Results of test drilling at Newberry Volcano, Oregon- and some implications for geothermal prospects in the Cascades: Geothermal Resources Council Bulletin, p. 3-8.
Sammel, E.A., and Craig, R.W., 1983, Hydrology of the Newberry Volcano Caldera, Oregon: U.S. Geological Survey Water Resources Investigation Report 83-4091, 52p.
Seki, Y., 1972, Lower grade stability limit of epidote in the light of natural occurrences: Journal of Geological Society of Japan, v. 78, p. 405-413.
Sheridan, M.F., and Maisano, M.D., 1976, Zeolite and sheet silicate zonation in a Late-Tertiary geothermal basin near Hassayampa, central Arizona: Proceedings of the 2nd U.N. Symposium on the Development and Use of Geothermal Resources, San Francisco, California, 20-29 May, 1975, v. 1, U.S. Government Printing Office, Washington D.C., p. 597-607.
Sigvaldson, G.E., and White, D.E., 1961, Hydrothermal alteration of rocks in two drill holes at Steamboat Springs, Washoe County, Nevada: U.S. Geological Survey Professional Paper 424-D, p. D116-D122.
Sigvaldson, G.E., and White, D.E., 1962, Hydrothermal alteration in drill holes GS-5 and GS-7, Steamboat Springs, Nevada: U.S. Geological Survey Professional Paper, 450-D, p. D113-D117.
Steiner, A., 1977, The Wairakei geothermal area, North Island, New Zealand: Its subsurface geology and hydrothermal rock alteration: New Zealand Geological Survey Bulletin 90, 136p.
Williams, H., 1957, A geologic map of the Bend quadrangle, Oregon and a reconaissance geologic map of the central portion of the High Cascade Mountains: Oregon Department of Geology and Mineral Industries Map, Scales 1:125,000, and 1:250,000.
Williams, H., 1935, Newberry volcano of central Oregon: Geological Society of America Bulletin, v. 46, p. 253-304.
Wise, W.S., 1982, New occurrence of faujasite in southeastern California: American Mineralogist, v. 67, p. 794-798.
Wise, W.S., and Tschernich, R.W., 1978, Dachiardite-bearing assemblages in the Pacific Northwest: In L.B. Sand, and F.A. Mumpton (eds.), Natural Zeolites: Occurrence, Properties, Use, Pergamon, New York, p. 105-111.

FIGURE CAPTIONS

Figure 1. Map of Newberry Caldera showing location of Newberry 2 geothermal drill hole, hot springs, fumaroles, and recent volcanic deposits.

2. Depth distribution of hydrothermal alteration minerals in lower two-thirds of Newberry 2 drill hole. Left column shows a generalized stratigraphic section of rock units encountered in drill hole (Sammel, 1981; MacLeod and Sammel, 1982). Horizontal lines in far right column indicates distribution of samples studied. Width of mineral columns gives approximation of relative mineral abundance based on X-ray-diffraction and microscope observation. Vertical continuity in mineral presence between samples studied assumed except where a mineral abundance becomes zero, in which case the zero point is arbitrarily placed 0.3 m from last occurrence of the mineral. Solid curve shows measured temperature profile from drill hole (Sammel, 1981; MacLeod and Sammel, 1982).

3. Scanning electron micrograph of a large trapezohedral analcime crystal from 315 m. Analcime deposited on altered glass composed of smectite or poorly crystalline zeolite material. Tiny bladed crystals deposited later than analcime were not identified. Scale on scanning electron micrographs is given as distance between white tick marks at bottom of micrographs (10 micrometers in Figure 3).

4. Scanning electron micrograph showing small, interpenetrating analcime crystals from 319 m that are deposited on altered glass (smectite, or poorly crystalline zeolitic material).

5. Scanning electron micrographs of chabazite from 309 m showing (a) tabular to blocky habit with some interpenetrating twins and slight flaking or desiccation, and (b) extensive flaking so that crystal form is no longer recognizable.

6. Scanning electron micrograph showing bladed to fibrous (?) habit of clinoptilolite from 442 m deposited later than smectite in altered pumiceous glass.

7. Scanning electron micrograph of fibrous to ribbon-like dachiardite crystals from 443 m.

8. Scanning electron micrograph showing fibrous habit of erionite from 315 m deposited on altered glass material consisting of smectite or or poorly crystalline zeolitic material.

9. Scanning electron micrograph showing twinned faujasite crystals deposited later than chabazite at 309 m.

10. Scanning electron micrograph showing cavity filling of fibrous mordenite at 496 m.

11. Scanning electron micrograph showing spherical cluster of platey gyrolite crystals from 306 m.

12. $CaCO_3$-$MgCO_3$-$FeCO_3$+$MnCO_3$ ternary diagram for microprobe chemical analyses of carbonate minerals from Newberry 2 drill hole.

13. Scanning electron micrograph of needle-like habit for calcite crystals from vein at 309 m.

14. Scanning electron micrograph of blocky crystals of calcite from 848 m.

15. Scanning electron micrographs showing (a) blocky rhombic dolomite-ankerite crystals from 739 m, and (b) disc-shaped and rectangular aggregates of rhombic dolomite-ankerite crystals from 694 m. A few hemispherical clusters of platey smectite clusters were deposited later than carbonate mineral in (b).
16. Scanning electron micrographs showing (a) disc-shaped aggregates siderite crystals from 566 m, and (b) spherical clusters of disc-shaped aggregates of siderite crystals from 572 m.
17. $CaCO_3$-$MgCO_3$+$FeCO_3$-$MnCO_3$ ternary diagram for microprobe chemical analyses between the core and rim of a spherical cluster of siderite crystals from 591 m. The two tracks of analyses (denoted by + and Δ) were made at ~90° angle.
18. Scanning electron micrograph showing tabular hexagonal apatite crystals from 910 m. Tiny chlorite tablets are deposited later than apatite.
19. Scanning electron micrograph showing hydrogrossular crystals that comprise entire pinkish sediment sample recovered from 315 m.
20. Scanning electron micrograph of trapezohedral hydrogrossular crystals from 315 m.
21. Scanning electron micrograph showing irregular sheet-like and stacks of platey crystals of smectite from 744 m.
22. Scanning electron micrograph showing spherical clusters of irregular sheet-like smectite crystals deposited on carbonate crystals at 690 m.
23. Scanning electron micrograph showing intergrowth of sheet-like illite crystals and tiny chlorite platey crystals from 908 m.
24. Scanning electron micrograph showing sheet-like mixed-layer chlorite-smectite from 894 m.
25. Scanning electron micrograph of rosettes of platy mixed-layer chlorite-smectite from 915 m.
26. Scanning electrton micrograph of radiating sheet-like crystals of chlorite from 741 m.
27. Scanning electron micrograph showing books of hexagonal platy chlorite crystals from 931 m.
28. Diagram showing ranges of secondary fluid inclusion filling temperatures in quartz crystals from 6 depths within the Newberry 2 drill hole. Dashed line is measured temperature curve (Sammel, 1981).
29. Scanning electron micrograph showing laminar hexagonal platelets of pyrrhotite crystals from 908 m.
30. Scanning electron micrograph of pyrite and marcasite pseudomorphous after pyrrhotite at 535 m.
31 Phase diagram for Fe-S system below 350°C (after Kissin and Scott, 1982) showing microprobe chemical composition of monoclinic pyrrhotite from 4 depths in Newberry 2 drill hole. Temperature data from Sammel (1981).
32. Scanning electron micrograph showing tabular marcasite crystals and smectite from 566 m. One crystal (at left-center of photo) appears to have "cockscomb" habit.

33. Scanning electron micrographs showing (a) interpenetration epidote crystals from 916 m, and (b) same as (a).
34. Scanning electron micrograph showing blocky anhydrite crystals on fracture surface at 902 m that are coated by later rosette clusters of chlorite-smectite.

Appendices. Electron microprobe analyses of carbonate and sulfide minerals. Analyses were made on an ARL electron microprobe using natural and synthetic mineral standards.

Appendix 1. Aragonite.

Sample No.	MgO	CaO	MnO	FeO	SrO	BaO	SiO_2
N1003.0-1	0.75	53.78	0.19	0.20	0.06	0.08	0.00
-2[1]	0.41	52.82	0.15	0.21	0.07	0.07	0.00
-3	0.26	51.38	0.09	0.17	0.05	0.11	0.00
-4	1.07	51.85	0.24	0.25	0.17	0.12	0.00

1 Average of 6 analyses.

Appendix 2. Calcite.

Sample No.	MgO	CaO	MnO	FeO	SrO	BaO	SiO_2
N1013.5-1	0.11	55.11	0.10	0.17	0.08	0.05	0.00
-2	0.16	54.35	0.15	0.20	0.04	0.12	0.00
-3	0.17	55.23	0.17	0.23	0.11	0.10	0.02
-4	0.16	55.75	0.13	0.21	0.00	0.04	0.02
-5	0.15	54.61	0.12	0.19	0.09	0.13	0.01
-6	0.16	55.57	0.11	0.15	0.03	0.16	0.02
-7	0.19	55.47	0.10	0.16	0.11	0.15	0.01
N1485.5-4	0.54	48.29	2.13	3.86	0.00	0.00	0.02
-5	0.59	48.38	2.08	3.77	0.00	0.03	0.00
-6	0.52	48.91	2.19	3.41	0.00	0.02	0.00
-7	0.50	44.04	5.08	3.71	0.00	0.00	0.01
-8	0.59	47.52	2.14	3.78	0.00	0.01	0.01
N2352.0-1	1.10	41.49	10.19	6.40	0.00	0.11	0.00
-2	1.06	42.48	9.62	6.20	0.01	0.13	0.02
-3	1.02	44.32	8.80	5.20	0.07	0.12	0.00
-4	1.07	39.68	8.92	7.57	0.00	0.10	0.01
-5	0.35	55.94	2.77	1.73	0.05	0.11	0.00
-6	0.31	57.27	1.14	0.60	0.01	0.13	0.00
-7	0.17	52.36	0.40	0.23	0.03	0.07	0.00
-8	0.35	53.86	3.10	1.57	0.04	0.15	0.11
-9	0.31	55.75	2.35	1.19	0.08	0.13	0.00

Sample No.	MgO	CaO	MnO	FeO	SrO	BaO	SiO_2
N2352.0-10	0.41	55.20	3.40	1.76	0.15	0.15	0.00
-11	1.21	41.04	9.96	6.69	0.15	0.10	0.00
-12	1.16	42.63	8.61	6.89	0.04	0.14	0.00
-13	0.76	46.84	7.17	4.28	0.07	0.11	0.03
-14	0.58	46.96	5.77	3.32	0.02	0.14	0.14
-15	0.07	48.19	6.98	4.09	0.03	0.08	0.01
-16	0.74	46.79	7.09	4.55	0.02	0.07	0.07
-17	0.56	50.95	7.45	3.70	0.09	0.10	0.06
-18	0.57	51.80	6.93	3.12	0.18	0.19	0.00
N2416.0-1	0.24	55.03	1.33	0.53	0.09	0.09	0.05
-2	0.28	55.96	1.87	0.56	0.08	0.11	0.15
-3	0.31	56.22	1.85	0.64	0.16	0.15	0.07
-4	0.31	54.75	2.30	0.73	0.01	0.10	0.05
-5	0.35	53.62	2.37	0.83	0.08	0.13	0.17
N2430.0-1	0.82	51.14	3.85	0.92	0.21	0.12	0.16
-2	1.00	54.38	3.68	1.05	0.09	0.04	0.00
-3	0.90	54.68	3.63	0.92	0.12	0.04	0.01
-4	0.94	54.60	3.67	0.99	0.17	0.05	0.00
-5	0.76	54.97	3.53	0.89	0.11	0.12	0.00
-6	0.93	54.32	3.60	0.95	0.11	0.09	0.00
-7	1.04	52.18	4.12	1.23	0.14	0.05	0.05
-8	0.91	54.87	3.40	1.02	0.18	0.09	0.01
-9	0.83	54.46	3.62	0.98	0.11	0.10	0.00
-10	0.86	54.50	3.50	1.05	0.24	0.07	0.00

Appendix 3. Dolomite-Ankerite.

Sample No.	MgO	CaO	MnO	FeO	SrO	BaO	SiO_2
N1362.0-1[1]	22.63	28.80	0.04	1.50	0.00	0.00	-
-2[2]	22.60	29.38	0.05	1.53	0.00	0.00	-
-3[3]	18.52	28.50	0.48	5.69	0.00	0.05	-
-4[2]	20.16	30.04	0.24	3.80	0.00	0.01	-
-5[3]	26.16	20.43	0.20	5.75	0.00	0.00	-
-6	22.70	29.63	0.00	1.54	0.00	0.01	-
-7	23.39	29.39	0.03	1.67	0.00	0.00	-
-9	23.14	27.81	0.00	1.78	0.00	0.04	-
-10	22.59	30.39	0.00	1.87	0.00	0.03	-
-11	21.02	27.16	0.16	4.80	0.00	0.02	-
-12	22.46	29.72	0.01	1.67	0.00	0.02	-
-13	22.79	29.29	0.03	1.64	0.00	0.00	-
-14	22.26	29.36	0.00	1.64	0.00	0.05	-
-15	22.16	29.56	0.14	1.86	0.00	0.00	-
-16	16.08	34.08	0.26	5.25	0.00	0.01	-
-17	22.19	29.34	0.18	1.89	0.07	0.06	0.02
-18	22.36	28.17	0.17	1.49	0.06	0.13	0.00
-19	23.88	27.91	0.21	2.44	0.10	0.12	0.00
-20	23.62	29.61	0.12	1.30	0.04	0.08	0.00
-21	23.21	29.03	0.14	1.73	0.10	0.05	0.00
-22	24.12	26.70	0.12	1.51	0.08	0.12	0.00

Sample No.	MgO	CaO	MnO	FeO	SrO	BaO	SiO_2
N1362.0-23	23.18	28.06	0.10	1.59	0.06	0.11	0.00
-24	22.93	29.67	0.17	1.73	0.06	0.08	0.00
-25	23.56	28.41	0.11	1.17	0.17	0.13	0.00
-26	23.59	28.23	0.08	1.59	0.06	0.07	0.00
-27	22.85	28.74	0.16	1.41	0.17	0.08	0.00
-28	23.62	28.66	0.11	1.37	0.00	0.09	0.00
-29	22.68	28.95	0.21	1.96	0.07	0.09	0.01
-30	23.46	28.67	0.10	1.52	0.04	0.03	0.00
-31	23.74	28.81	0.18	1.88	0.07	0.12	0.00
-32	23.86	28.10	0.17	1.76	0.04	0.07	0.00
-33	23.14	29.34	0.13	1.32	0.12	0.07	0.00
-34	22.73	29.37	0.11	1.44	0.10	0.05	0.00
-35	23.11	28.30	0.13	1.31	0.12	0.02	0.00
-36	22.62	29.15	0.09	1.25	0.18	0.10	0.00
-37	21.67	29.42	0.15	1.59	0.14	0.09	0.20
-38	22.41	28.99	0.19	1.89	0.13	0.08	0.00
-39	22.71	29.35	0.17	1.85	0.07	0.07	0.00
-40	22.58	29.27	0.20	1.82	0.09	0.08	0.03
-41	21.64	29.16	0.18	1.63	0.03	0.13	0.10
-42	22.34	28.75	0.13	1.63	0.07	0.04	0.01
-43	22.81	29.27	0.17	1.96	0.17	0.10	0.00
-44	21.73	28.91	0.25	2.57	0.06	0.09	0.00
-45	21.92	28.96	0.27	3.20	0.07	0.11	0.00

Sample No.	MgO	CaO	MnO	FeO	SrO	BaO	SiO_2
N1362.0-46	22.87	28.95	0.13	1.76	0.00	0.11	0.00
-48	23.54	28.81	0.11	2.07	0.02	0.04	0.00
-50	26.79	21.67	0.22	3.57	0.02	0.07	0.00
-51	22.80	29.64	0.18	1.71	0.07	0.16	0.00
-52	20.26	27.46	0.36	5.27	0.05	0.10	0.00
-53	22.69	30.05	0.19	2.19	0.13	0.13	0.00
-54	17.02	32.41	0.35	6.05	0.04	0.12	0.01
-55	16.97	30.67	0.35	6.35	0.00	0.07	0.00
-56	16.65	31.75	0.39	5.95	0.07	0.05	0.00
-57	20.67	31.32	0.24	3.48	0.06	0.10	0.02
-58	17.23	32.77	0.42	6.10	0.00	0.08	0.00
-59	20.61	30.77	0.20	3.34	0.07	0.11	0.00
-60	19.38	32.22	0.19	2.98	0.06	0.08	0.01
-61	17.63	31.21	0.39	6.17	0.12	0.08	0.00
-62	17.16	31.50	0.36	5.86	0.07	0.08	0.00
-63	16.69	30.78	0.36	5.84	0.02	0.13	0.00
-64	17.45	30.94	0.36	5.82	0.00	0.06	0.00
-65	16.91	31.84	0.29	6.21	0.02	0.10	0.00
-66	22.38	29.79	0.27	2.54	0.03	0.09	0.00
-67	23.67	26.04	0.15	2.45	0.05	0.02	0.00
-68	27.71	22.16	0.22	3.18	0.11	0.06	0.00
-69	23.27	28.69	0.13	1.87	0.08	0.05	0.03
-70	22.18	28.99	0.18	2.21	0.03	0.14	0.00
-72	22.46	28.80	0.15	1.40	0.02	0.00	

Sample No.	MgO	CaO	MnO	FeO	SrO	BaO	SiO_2
N1362.0-74	22.61	27.71	0.24	2.28	0.12	0.12	0.10
-75	16.79	31.19	0.32	6.59	0.01	0.12	0.00
-76	16.45	31.63	0.31	5.97	0.04	0.10	0.00
-77	15.76	34.31	0.38	5.32	0.09	0.03	0.00
-78	15.98	30.77	0.41	6.76	0.00	0.03	0.00
-79	15.07	34.60	0.43	5.71	0.03	0.10	0.00
-80	14.45	31.33	0.67	8.37	0.06	0.11	0.00
-81	23.54	29.30	0.12	1.50	0.10	0.04	0.00
N2265.0-1	16.68	29.35	1.04	4.03	0.00	0.03	0.04
-2	17.15	28.25	0.63	5.11	0.00	0.00	0.02
-9	17.25	28.90	0.68	3.88	0.00	0.00	0.00
N2276.0-3	16.45	28.53	0.81	7.88	0.00	0.04	0.00
-4	19.54	29.63	0.36	4.54	0.04	0.11	0.04
-7	18.27	30.65	0.31	5.08	0.02	0.01	0.02
-8	16.46	28.14	0.67	8.32	0.08	0.07	0.12
-16	18.21	32.09	0.26	4.15	0.03	0.08	0.00
-20	17.72	28.34	0.50	7.01	0.04	0.11	0.00

[1] Average of 6 analyses.

[2] Average of 7 analyses.

[3] Average of 5 analyses.

Appendix 4. Magnesite.

Sample No.	MgO	CaO	MnO	FeO	SrO	BaO	SiO_2
N1362.0-8	43.68	3.72	0.00	1.25	0.00	0.00	-
-47	38.82	7.03	0.21	4.10	0.00	0.14	0.00
-49	42.31	4.07	0.18	3.01	0.00	0.08	0.00
-73	41.64	3.76	0.18	3.12	0.04	0.05	0.31

Appendix 5. Siderite.

Sample No.	MgO	CaO	MnO	FeO	SrO	BaO	SiO_2
N1362.0-71	3.36	2.99	1.31	52.01	0.04	0.11	0.02
N1477.0-1	3.74	4.62	3.68	45.75	0.00	0.00	0.84
-2	4.10	4.75	2.27	45.00	0.00	0.01	0.88
-4	4.89	8.24	6.50	36.85	0.00	0.05	0.05
-5	3.30	6.43	1.77	45.98	0.00	0.07	0.56
-6	3.73	6.63	2.38	43.77	0.00	0.03	0.27
-7	7.15	7.50	1.67	39.62	0.00	0.03	0.01
-8	7.37	6.87	1.47	40.03	0.00	0.00	0.02
-9	5.33	8.62	1.64	40.39	0.00	0.03	0.03
-10	3.18	8.84	1.30	42.46	0.00	0.08	0.04
-11	6.63	8.40	2.00	39.75	0.00	0.05	0.08
-12	5.20	8.29	1.47	41.72	0.00	0.11	0.27
-13	4.39	6.43	3.64	42.33	0.00	0.00	0.59
-14	3.34	8.22	1.12	44.61	0.00	0.11	0.14
-15	7.09	8.45	3.37	38.11	0.00	0.00	0.04
-16	6.40	8.03	3.39	39.25	0.00	0.07	0.21
-17	4.82	8.05	1.89	43.10	0.00	0.10	0.00
-18	4.26	7.65	2.57	43.80	0.00	0.07	0.14
-19	6.65	8.68	1.82	40.45	0.00	0.09	0.00
-20	4.28	7.37	2.33	42.85	0.00	0.02	0.91
-21	4.04	8.01	2.21	43.80	0.00	0.00	0.01
-22	4.08	8.13	2.87	42.84	0.00	0.05	

Sample No.	MgO	CaO	MnO	FeO	SrO	BaO	SiO_2
N1485.5-1	6.15	9.02	1.05	37.86	0.00	0.02	0.02
-2	5.71	9.19	1.10	38.44	0.00	0.02	0.04
-3	5.26	8.92	1.09	39.11	0.00	0.04	0.01
-9	5.67	8.52	1.07	38.19	0.00	0.08	0.01
-10	6.03	8.62	1.12	38.21	0.00	0.06	0.00
-11	6.23	8.40	1.10	37.64	0.00	0.06	0.03
-12	6.16	8.86	1.08	38.21	0.00	0.03	0.04
-13	5.90	8.20	1.08	39.45	0.00	0.04	0.00
N1520.5-1	3.53	0.77	2.25	47.70	0.00	0.05	0.02
-2	3.86	0.37	1.90	48.55	0.00	0.01	0.00
-3	3.27	1.01	2.34	48.37	0.00	0.09	0.00
-4	3.25	0.87	2.24	48.62	0.00	0.05	0.03
-5	3.35	0.87	2.20	48.70	0.00	0.08	0.00
-6	3.47	0.80	2.25	48.03	0.00	0.03	0.01
-7	3.35	0.87	2.36	48.17	0.00	0.08	0.04
-8	3.32	0.88	2.24	47.72	0.00	0.07	0.01
-9	3.52	0.78	2.22	48.42	0.00	0.08	0.00
-10	3.77	0.73	2.37	47.94	0.00	0.03	0.00
N1856.0-1[1]	8.28	4.73	2.65	44.57	0.00	0.06.	-
-2[2]	6.20	5.34	4.04	44.71	0.00	0.09	-
-3[2]	5.53	3.95	3.04	48.14	0.00	0.09	-
-4[2]	6.24	5.65	4.12	44.17	0.00	0.09	-
N1867.0-1	6.51	4.49	3.50	42.51	0.00	0.05	0.11
-2	7.90	5.19	4.65	39.21	0.00	0.04	0.25

Sample No.	MgO	CaO	MnO	FeO	SrO	BaO	SiO_2
N1867.0-3	7.81	6.18	3.42	39.70	0.00	0.04	0.00
-4	6.40	4.45	3.57	42.66	0.00	0.01	0.02
-5	5.49	3.38	3.76	44.78	0.00	0.02	0.03
-6	7.74	5.44	3.51	37.94	0.00	0.03	2.04
-7	9.42	3.50	1.85	41.90	0.00	0.01	0.00
-8	8.34	5.56	3.92	38.55	0.00	0.07	0.02
-9	5.79	3.47	2.49	45.58	0.00	0.05	0.01
-10	5.89	3.68	2.65	45.54	0.00	0.11	0.02
N1870.0-1	9.75	4.42	2.17	41.18	0.00	0.04	0.03
-2	9.71	3.69	1.68	42.39	0.00	0.04	0.00
-3	8.57	4.49	2.24	42.38	0.00	0.09	0.03
-4	9.26	3.26	2.22	42.99	0.00	0.02	0.01
-5	2.56	8.08	12.38	35.27	0.00	0.05	0.04
-6	2.82	8.44	7.93	39.85	0.00	0.11	0.01
-7	4.30	6.59	5.80	40.83	0.00	0.08	0.15
-8	2.28	7.84	11.66	36.91	0.00	0.07	0.07
-9	3.07	7.00	10.40	37.65	0.00	0.01	0.32
-10	2.81	8.54	7.41	39.44	0.00	0.06	0.04
-11	8.28	8.41	6.45	33.42	0.00	0.04	0.02
-12	5.82	5.11	2.96	42.12	0.00	0.07	1.23
-13	3.35	8.08	4.89	41.84	0.00	0.03	0.01
-14	4.71	7.25	3.74	42.52	0.00	0.04	0.02
-15	4.34	6.26	3.39	43.66	0.00	0.06	1.03
-16	4.63	4.64	2.77	45.96	0.00	0.00	0.68

Sample No.	MgO	CaO	MnO	FeO	SrO	BaO	SiO_2
N1870.0-17	5.77	3.07	2.66	46.50	0.00	0.04	0.37
-18	5.83	3.11	2.60	46.49	0.00	0.04	0.47
N1937.5-4	1.39	8.99	15.31	32.43	0.00	0.01	0.25
-5	2.31	9.27	6.45	39.88	0.00	0.09	0.04
-6	3.02	10.27	5.29	39.53	0.00	0.03	0.01
-7	6.27	7.83	2.81	40.22	0.00	0.06	0.02
-8	5.60	4.35	2.59	45.59	0.00	0.07	0.00
-9	7.05	6.06	4.18	40.32	0.00	0.05	0.09
-10	5.77	3.55	3.61	46.23	0.00	0.07	0.01
-11	6.97	6.11	2.62	42.77	0.00	0.05	0.02
-12	7.22	4.40	3.40	42.84	0.00	0.05	0.04
-17	0.80	12.44	14.69	30.56	0.00	0.09	0.03
-18	1.93	9.70	8.17	38.26	0.00	0.08	0.01
-19	2.13	10.06	8.92	36.86	0.00	0.07	0.02
-20	4.45	8.57	3.50	40.75	0.00	0.07	0.02
-21	7.40	7.46	3.20	38.27	0.00	0.14	0.02
-22	6.70	6.31	4.64	40.36	0.00	0.03	0.01
-23	7.86	4.59	3.19	42.24	0.00	0.04	0.02
N2265.0-3	7.69	3.63	1.48	45.14	0.00	0.05	0.01
-4	11.25	7.15	0.47	36.50	0.00	0.05	0.03
-5	7.25	4.24	0.75	45.08	0.00	0.06	0.01
-6	7.70	4.01	1.01	45.01	0.00	0.08	0.01
-7	8.88	4.00	2.30	42.89	0.00	0.00	0.05
-8	13.85	5.84	2.16	34.32	0.00	0.00	0.00

Sample No.	MgO	CaO	MnO	FeO	SrO	BaO	SiO_2
N2265.0-10	7.32	3.38	1.73	45.53	0.00	0.05	0.00
-11	9.54	3.97	1.03	41.89	0.00	0.02	0.00
-12	8.91	3.67	2.21	42.77	0.00	0.06	0.01
-13	8.29	4.06	1.33	44.22	0.00	0.10	0.00
-14	9.79	3.84	1.90	41.97	0.00	0.02	0.01
-15	10.63	3.91	2.27	40.03	0.00	0.04	0.01
-16	7.40	3.50	1.66	45.06	0.00	0.06	0.02
-17	7.57	3.91	1.09	45.55	0.00	0.06	0.02
N2276.0-1	8.26	4.12	1.39	43.85	0.07	0.12	0.00
-2	11.07	4.48	1.32	40.93	0.07	0.16	0.00
-5	12.12	2.53	2.02	40.97	0.08	0.13	0.07
-6	9.86	4.38	2.45	41.64	0.04	0.09	0.03
-9	10.22	4.63	2.56	40.03	0.03	0.07	0.01
-10	11.27	4.62	2.47	39.33	0.07	0.19	0.00
-11	12.71	5.03	2.04	37.89	0.01	0.13	0.06
-12	8.09	3.94	1.25	46.00	0.00	0.15	0.00
-13	9.15	4.50	2.33	42.11	0.04	0.10	0.00
-14	7.79	3.61	1.58	46.24	0.01	0.12	0.02
-15	7.66	4.11	1.09	46.19	0.07	0.15	0.00
-17	8.40	4.12	1.34	44.64	0.11	0.21	0.00
-18	10.04	4.25	4.63	38.70	0.09	0.17	0.00
-19	10.14	4.23	1.03	43.08	0.04	0.14	0.00
-21	9.71	4.27	1.80	42.66	0.04	0.16	0.00

Sample No.	MgO	CaO	MnO	FeO	SrO	BaO	SiO_2
N2276.0-22	7.58	3.70	1.50	46.05	0.06	0.11	0.00
-23	7.79	3.78	1.16	46.39	0.01	0.11	0.00
-24	8.37	4.30	1.31	43.89	0.07	0.11	0.00

1 Average of 7 analyses.

2 Average of 6 analyses.

Appendix 6. Calcium-, iron- rhodochrosite(?)

Sample No.	MgO	CaO	MnO	FeO	SrO	BaO	SiO_2
N1937.5-1	0.47	16.02	29.74	9.13	0.00	0.05	0.06
-2	1.16	9.49	21.54	18.20	0.00	0.00	0.35
-3	0.76	14.21	28.59	13.78	0.00	0.05	0.05
-13	0.43	16.31	30.15	7.15	0.00	0.02	0.22
-14	0.48	16.15	30.18	8.42	0.00	0.01	0.07
-15	0.41	11.11	24.94	16.89	0.00	0.03	1.99
-16	0.45	11.46	21.91	16.80	0.00	0.09	3.78

Appendix 7. Pyrrhotite.

Sample No.	S	Fe	Co	Ni	Total	No. Anal. Points	Atomic % Fe
N1520.5-3	38.30	56.47	0.03	0.00	94.80	5	45.83
-8	38.42	56.36	0.08	0.00	94.86	1	45.69
-9	38.34	56.69	0.03	0.00	95.06	1	45.90
-10	38.35	56.79	0.06	0.00	95.20	1	45.93
-11	38.49	56.84	0.03	0.00	95.36	1	45.87
-12	38.81	56.43	0.07	0.00	95.31	1	45.48
N2341.5-1	39.69	59.64	0.06	0.00	99.39	5	46.29
-2	39.64	59.38	0.04	0.00	99.06	1	46.22
-3	39.56	59.59	0.06	0.00	99.22	1	46.35
-4	39.47	59.97	0.04	0.02	99.50	1	46.57
-5	39.45	60.12	0.08	0.00	99.65	1	46.64
-6	39.93	60.12	0.02	0.00	100.07	1	46.36
-7	39.80	59.73	0.04	0.00	99.57	1	46.27
N2416.0-1	40.02	60.17	0.06	0.00	100.25	5	46.31
-2	38.95	59.50	0.05	0.00	98.50	1	46.71
-3	39.98	59.77	0.01	0.01	99.77	1	46.18
-4	39.39	60.45	0.02	0.03	99.89	1	46.82
-5	39.40	59.74	0.02	0.00	99.16	1	46.54
-6	40.03	59.86	0.02	0.03	99.94	1	46.18
-7	39.80	59.95	0.06	0.01	99.82	1	46.35
-8	39.85	59.91	0.03	0.00	99.79	1	46.32

Sample No.	S	Fe	Co	Ni	Total	No. Anal. Points	Atomic % Fe
N2416.0-8	39.85	59.91	0.03	0.00	99.79	1	46.32
-9	39.81	59.95	0.02	0.00	99.78	1	46.36
-10	39.42	60.30	0.03	0.00	99.75	5	46.74
-11	39.81	59.79	0.04	0.00	99.64	5	46.29
N2430.0-1	39.71	60.03	0.03	0.00	99.77	6	46.45
-2	39.87	60.02	0.09	0.02	100.00	1	46.32
-3	39.36	60.32	0.02	0.00	99.70	1	46.80
-4	40.06	60.20	0.05	0.00	100.31	1	46.30
-5	39.73	60.70	0.05	0.00	100.48	1	46.71
-6	38.88	59.85	0.06	0.00	98.79	1	46.89
-7	39.76	59.83	0.04	0.00	99.63	5	46.34

Appendix 8. Pyrite.

Sample No.	S	Fe	Co	Ni	Total	No. Anal. Points
N1477.0-1	51.05	45.46	0.00	0.00	96.51	6
-2	51.55	45.36	0.01	0.00	96.92	5
-3	51.65	45.08	0.00	0.00	96.73	1
-4	51.53	45.04	0.00	0.00	96.57	1
-5	51.57	45.60	0.02	0.00	97.19	1
-6	50.67	45.74	0.03	0.00	96.44	1
-7	51.04	45.67	0.02	0.00	96.73	5
-8	51.89	45.42	0.00	0.00	97.31	5
-9	51.48	45.50	0.01	0.00	96.99	5
-10	51.99	45.95	0.03	0.00	97.97	1
-11	51.90	45.68	0.01	0.00	97.59	1
-12	51.59	46.12	0.00	0.00	97.71	1
-13	50.53	46.05	0.00	0.00	96.58	1
-14	51.83	45.43	0.05	0.00	97.31	1
N1520.5-1	51.25	43.32	0.00	0.00	94.57	1
-2	51.24	42.82	0.00	0.00	94.06	6
-4	51.91	43.09	0.00	0.00	95.00	1
-5	50.76	43.42	0.00	0.00	94.18	1
-6	50.51	43.42	0.00	0.00	93.93	1
-7	50.08	43.41	0.00	0.00	93.49	1
N2276.0-1	51.70	45.84	0.04	0.00	97.58	5

Sample No.	S	Fe	Co	Ni	Total	No. Anal. Points
N2276.0-2	51.84	46.09	0.03	0.00	97.97	5
-3	52.47	46.40	0.01	0.00	98.88	5
-4	53.15	46.41	0.04	0.00	99.60	1
-5	52.73	45.87	0.01	0.00	98.61	1
-6	53.05	45.68	0.02	0.00	98.75	1
-7	52.13	45.81	0.00	0.00	97.94	1
N2352.0-1	52.89	46.10	0.06	0.00	99.05	5
-2	52.74	46.30	0.01	0.00	99.05	5
-3	52.89	46.49	0.02	0.00	99.40	1
-4	53.11	46.30	0.09	0.00	99.50	1
-5	53.13	46.70	0.00	0.00	99.83	1
-6	52.84	46.57	0.00	0.00	99.41	1
-7	52.32	46.82	0.03	0.00	99.17	1
N2378.8-1	52.78	46.44	0.01	0.00	99.23	5
-2	52.69	46.29	0.03	0.00	99.01	5
-3	52.10	45.41	0.04	0.00	97.55	1
-4	51.16	45.66	0.04	0.00	96.86	1
-5	52.10	46.14	0.14	0.00	98.38	1
-6	51.98	46.69	0.02	0.00	97.69	1
-7	52.06	45.82	0.01	0.00	97.89	1
N3051.5-1	53.36	46.36	0.07	0.00	99.79	5
-2	53.36	46.37	0.03	0.00	99.76	5
-3	52.38	45.82	0.07	0.00	98.27	1

Sample No	S	Fe	Co	Ni	Total	No. Anal. Points
N3051.5-4	53.69	46.03	0.01	0.00	99.82	1
-5	53.98	46.42	0.06	0.00	100.46	1
-6	51.37	44.53	0.03	0.00	95.93	1
-7	52.79	45.92	0.01	0.00	98.73	1

Appendix 9. Marcasite.

Sample No.	S	Fe	Co	Ni	Total	No. Anal. Points
N1856.0-1	52.81	46.41	0.00	0.00	99.22	9
-2	52.63	46.25	0.00	0.00	99.88	6
-3	53.19	46.15	0.00	0.00	99.34	1
-4	52.17	46.27	0.00	0.00	98.44	1
-5	53.11	46.46	0.00	0.00	99.57	1
-6	52.64	46.00	0.00	0.00	98.64	1
-7	52.29	45.99	0.00	0.00	98.28	1
-8	52.91	46.39	0.00	0.00	99.30	5
-9	52.18	46.24	0.00	0.00	98.42	5

Figures. Scanning electron micrographs (SEM) are provided by R.L. Oscarson. The scale for SEM's is given as distance between white tick marks at the bottom of the micrographs.

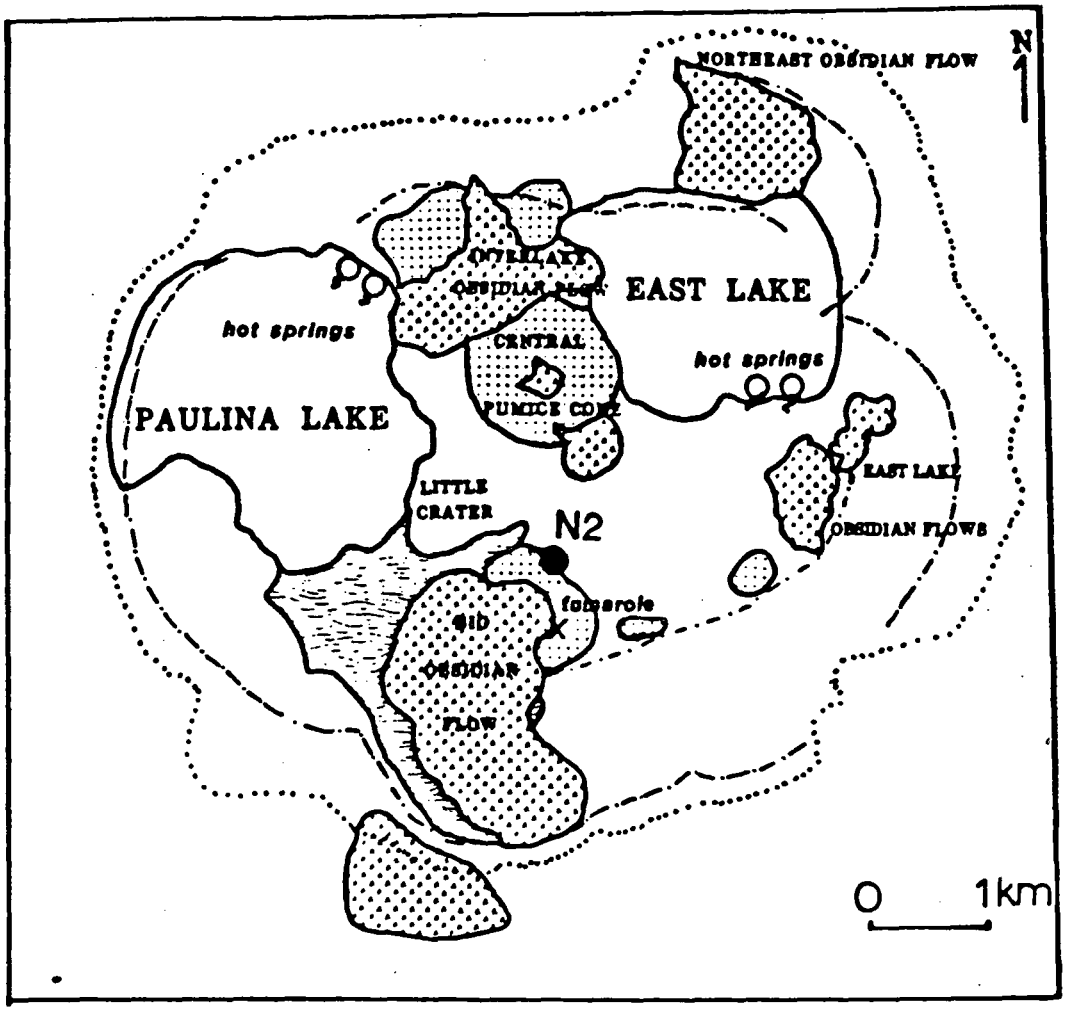
NORTHEAST OBSIDIAN FLOW
N
EAST LAKE
hot springs
CENTRAL
PUMICE CONE
hot springs
PAULINA LAKE
EAST LAKE
OBSIDIAN FLOWS
LITTLE
CRATER
N2
fumarole
OBSIDIAN
FLOW
0
1km

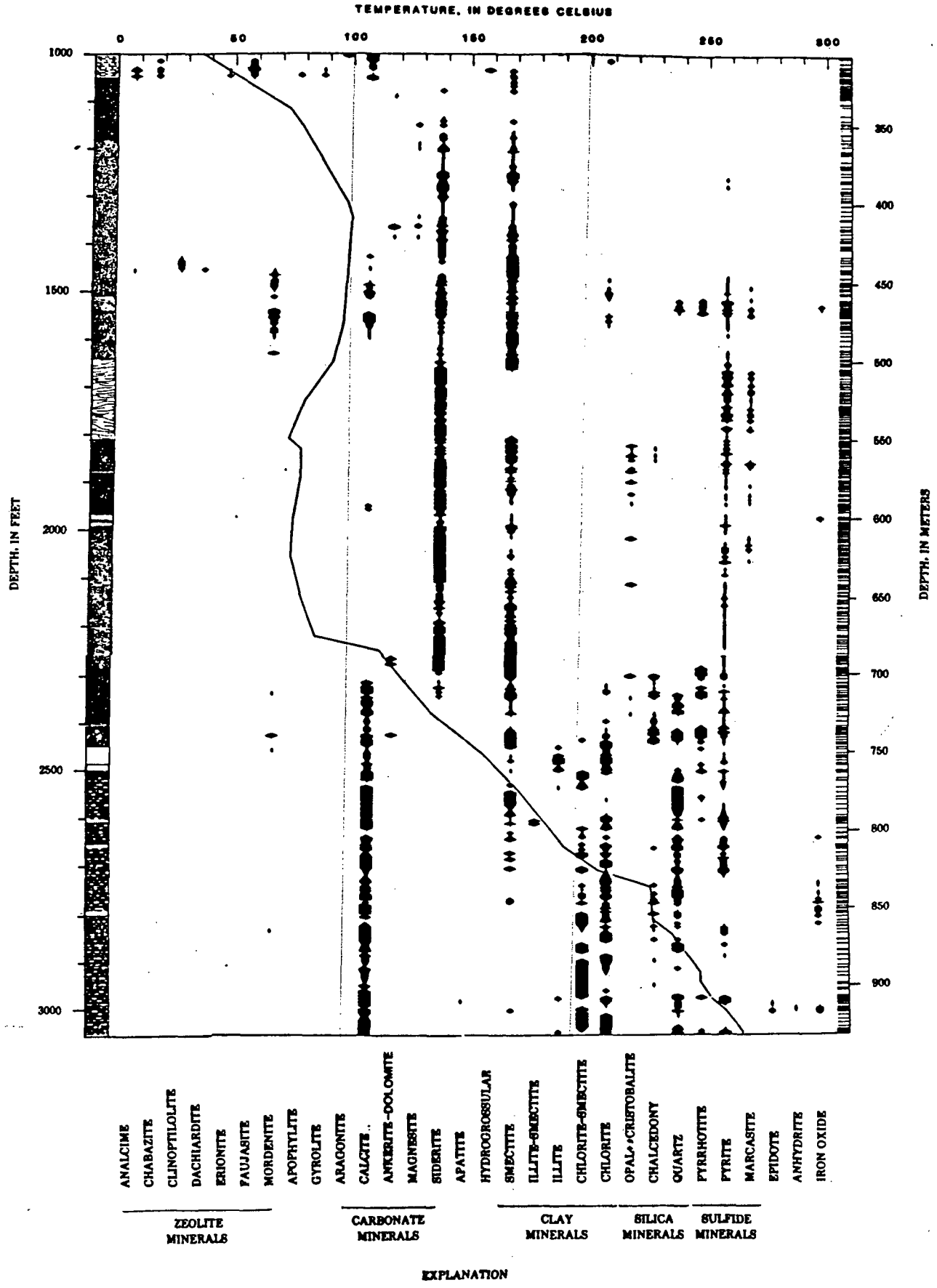
TEMPERATURE, IN DEGREES CELSIUS
0
50
100
150
200
250
300
DEPTH, IN FEET
1000
1500
2000
2500
3000
DEPTH, IN METERS
350
400
450
500
550
600
650
700
750
800
850
900
ANALCIME
CHABAZITE
CLINOPTILOLITE
DACHIARDITE
ERIONITE
FAUJASITE
MORDENITE
APOPHYLLITE
GYROLITE
ARAGONITE
CALCITE
ANKERITE-DOLOMITE
MAGNESITE
SIDERITE
APATITE
HYDROGROSSULAR
SMECTITE
ILLITE-SMECTITE
ILLITE
CHLORITE-SMECTITE
CHLORITE
OPAL-A/CRISTOBALITE
CHALCEDONY
QUARTZ
PYRRHOTITE
PYRITE
MARCASITE
EPIDOTE
ANHYDRITE
IRON OXIDE
ZEOLITE MINERALS
CARBONATE MINERALS
CLAY MINERALS
SILICA MINERALS
SULFIDE MINERALS
EXPLANATION
BASALTIC SEDIMENT
RHYOLITIC PUMICEOUS SEDIMENT
RHYOLITIC TUFF AND
RHYODACITE SILL
RHYODACITE FLOW
DACITE FLOW
ANDESITE FLOW
ANDESITIC TUFFACEOUS SEDIMENT
BASALT OR BASALTIC ANDESITE FLOWS

3

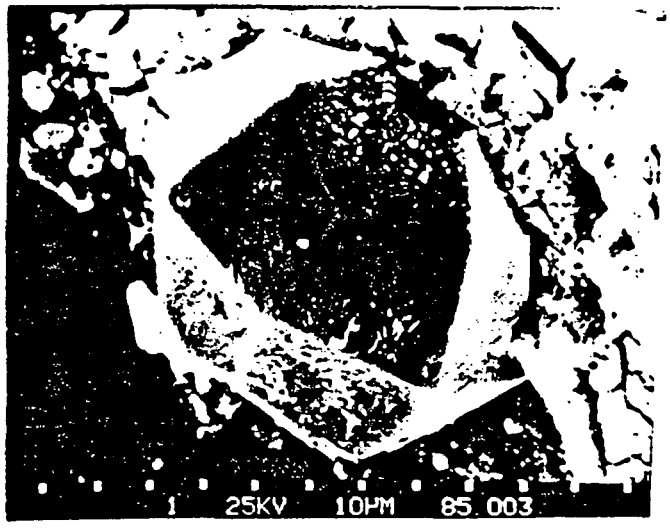
1 25KV 10μM 85.003

4

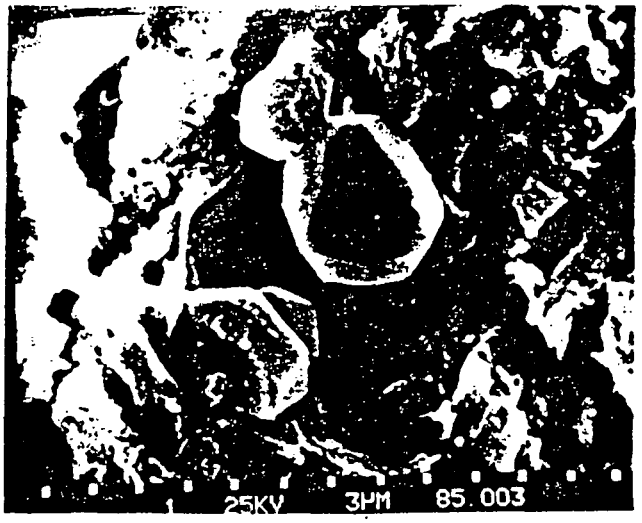
25KV 3μM 85.003

5A

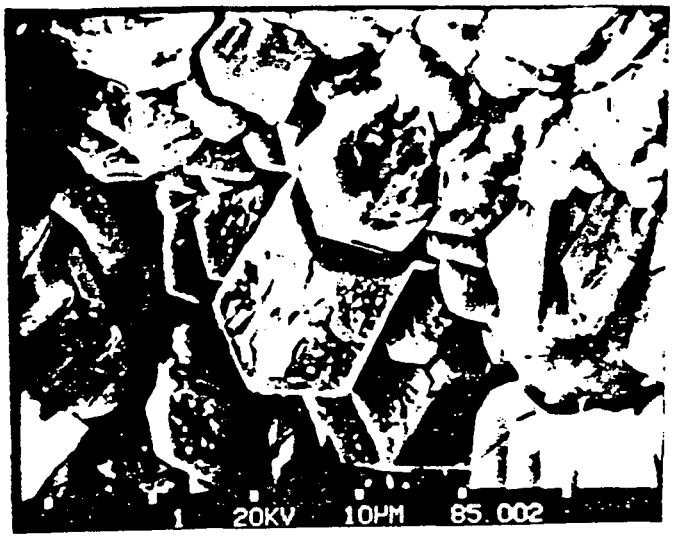
1 20KV 10μM 85.002

5B

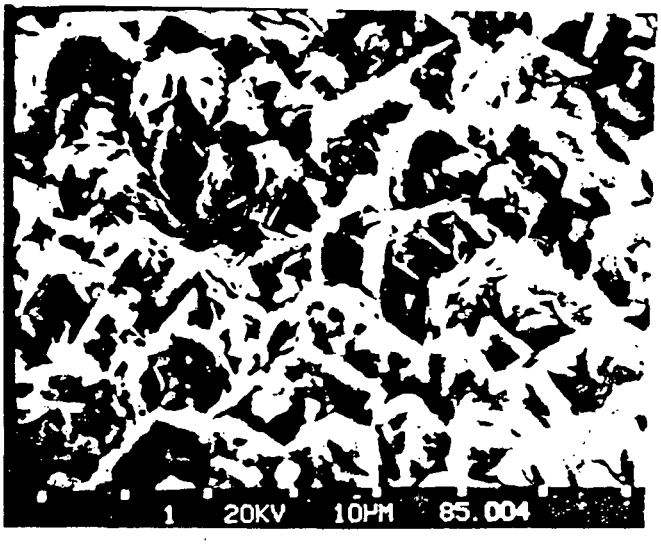
1 20KV 10μM 85.004

6

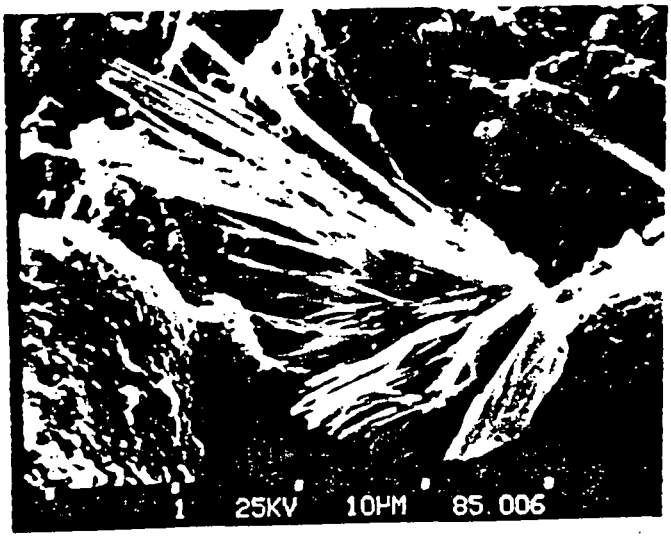
1 25KV 10μM 85.006

7

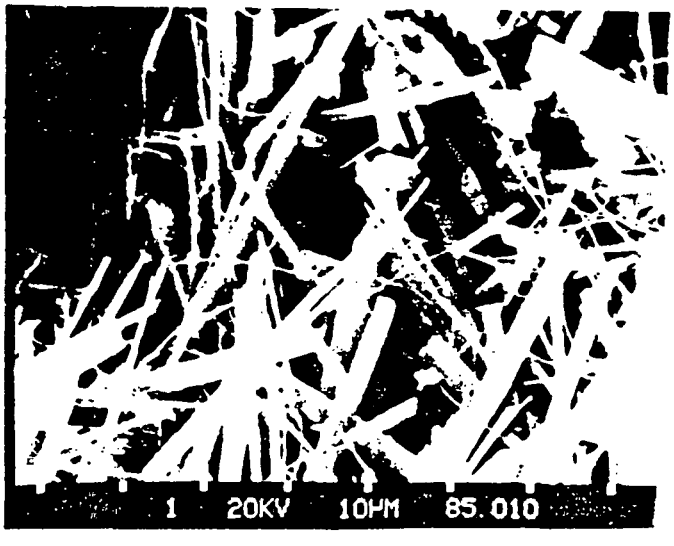
1 20KV 10μM 85.010

8

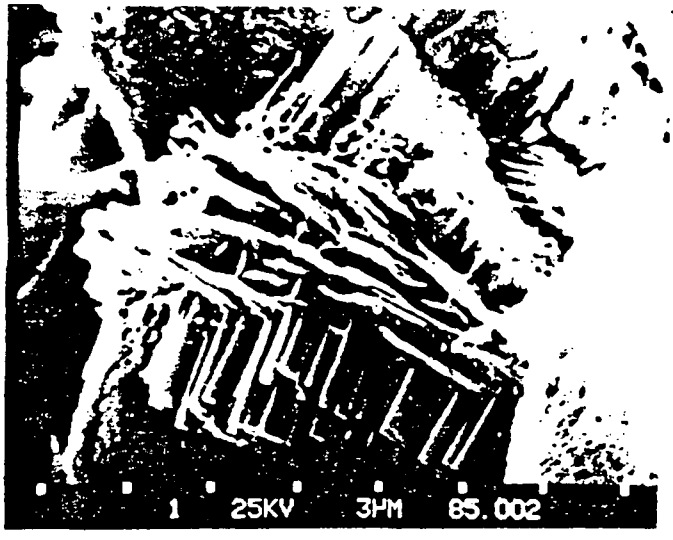
1 25KV 3μM 85.002

9


1 20KV 10μM 85.003

10

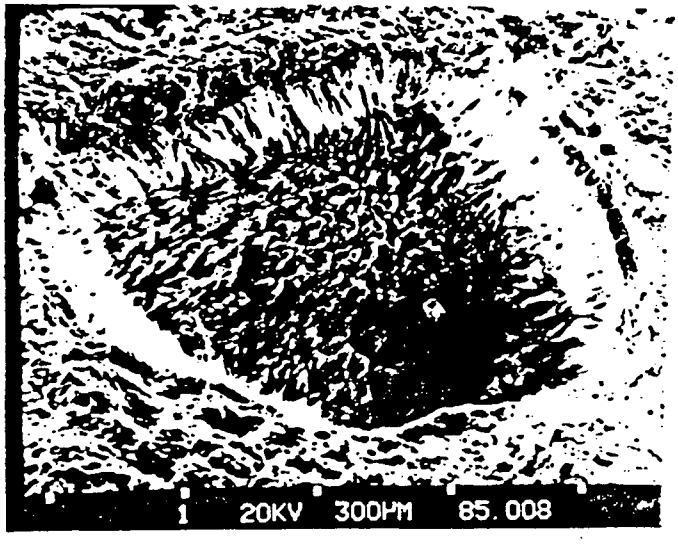
1 20KV 300μM 85.008

11

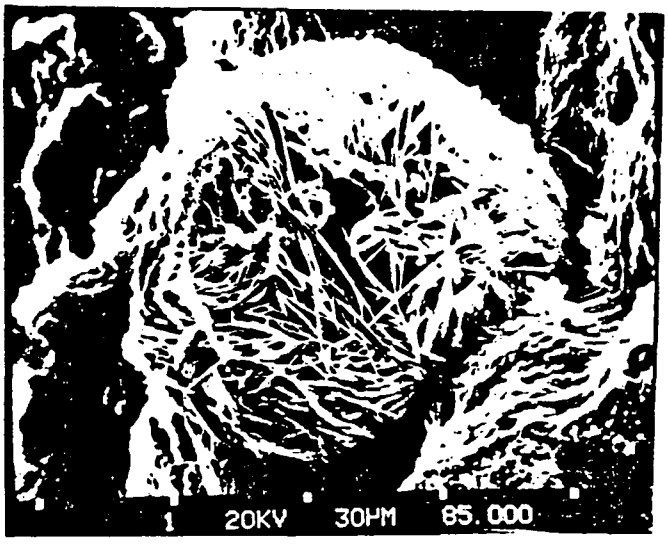
1 20KV 30μM 85.000

13

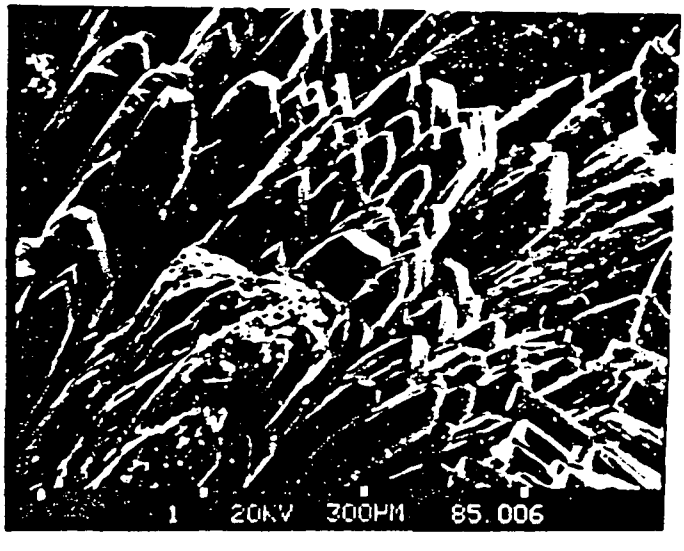
1 20KV 300μM 85.006

14

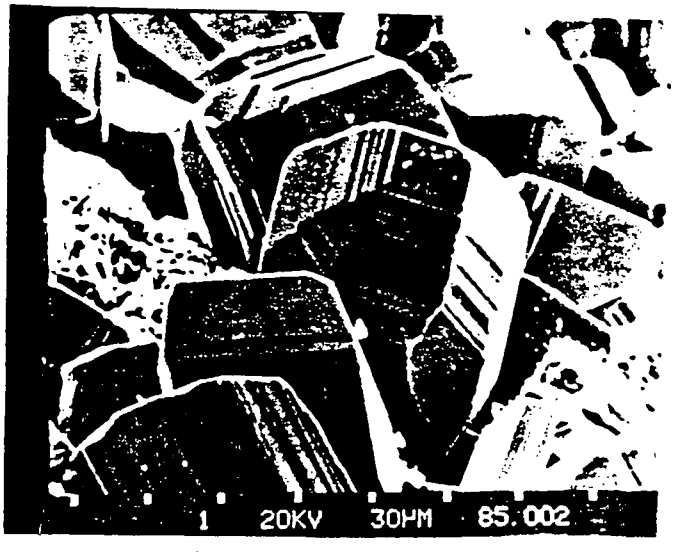
1 20KV 30μM 85.002

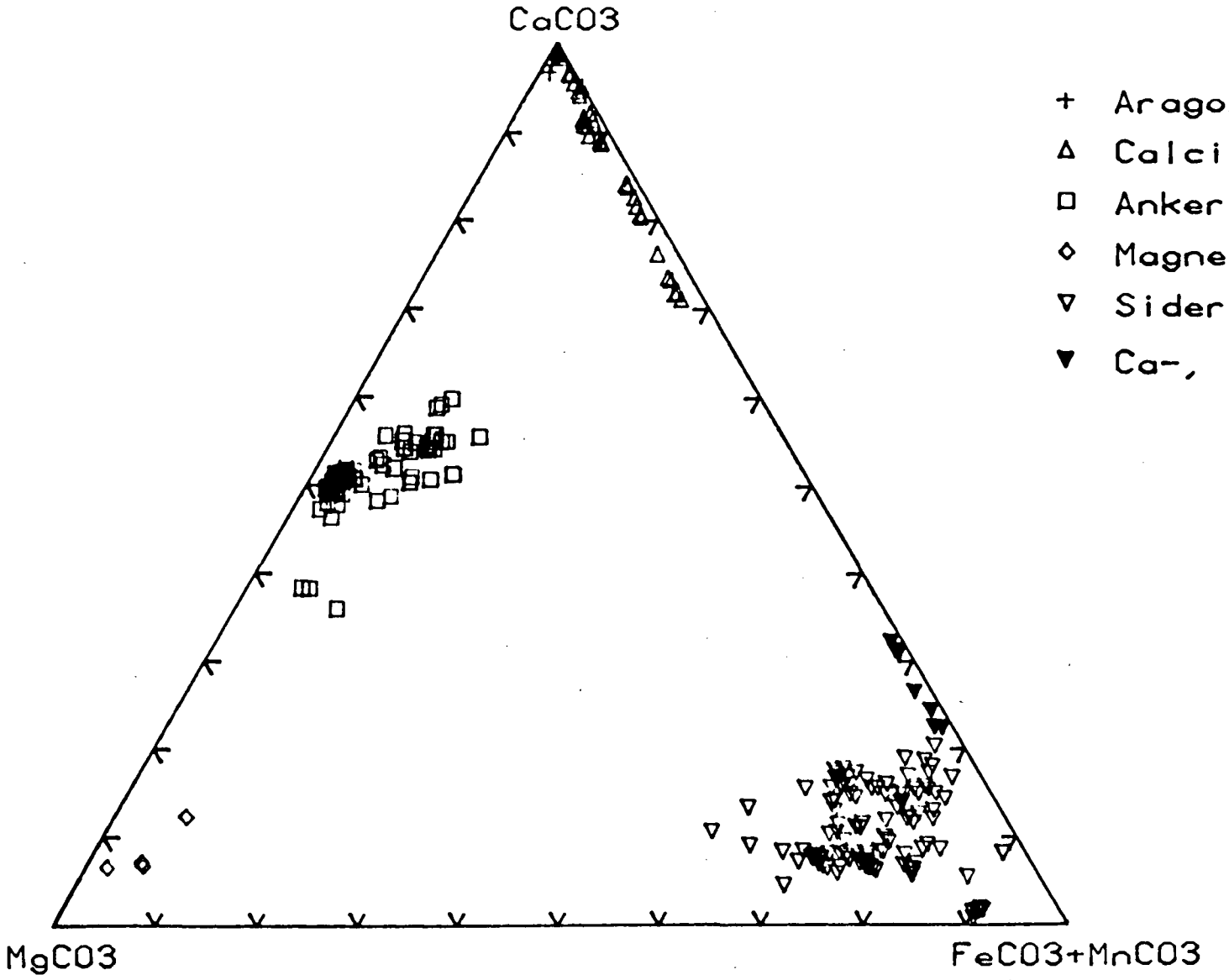

+ Aragonite
△ Calcite
□ Ankerite-Dolomite
◇ Magnesite
▽ Siderite
▼ Ca-, Fe- Rhodochrosite

15A

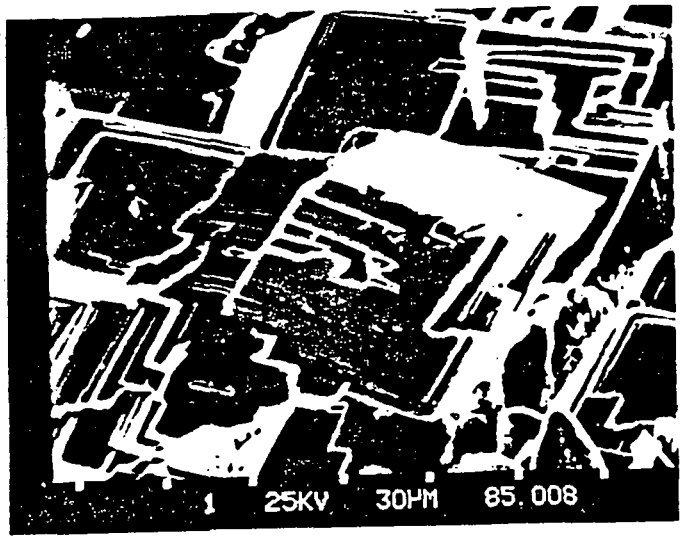

15B

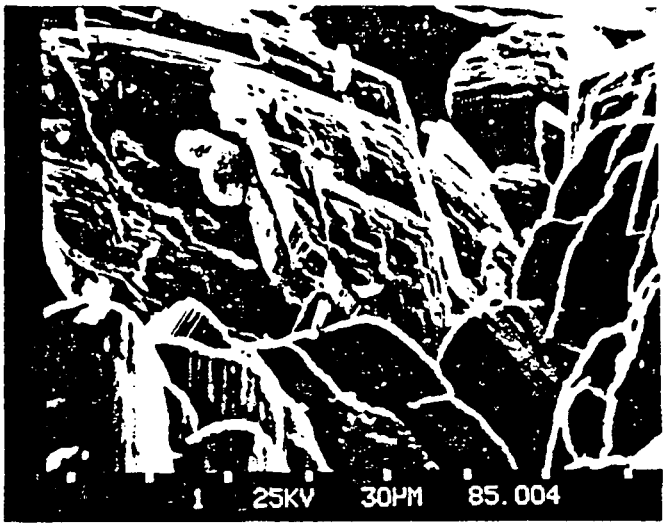

16A

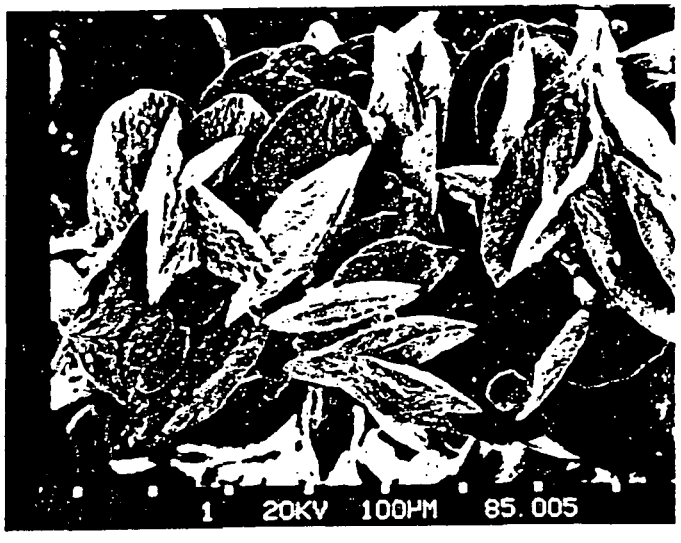

16B

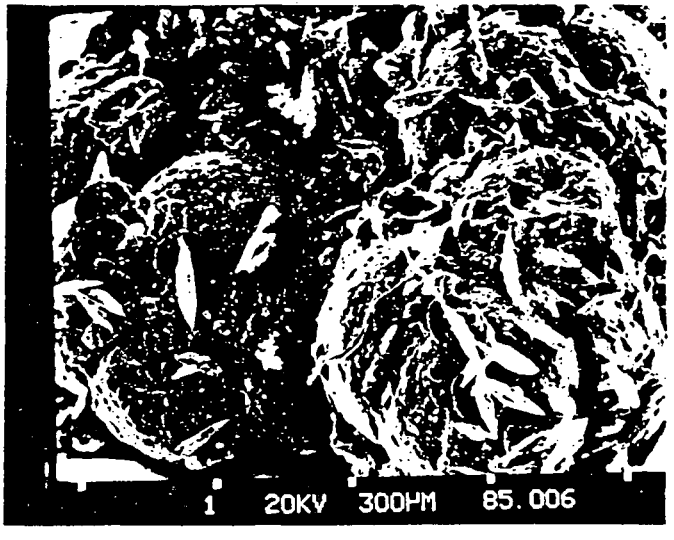

18

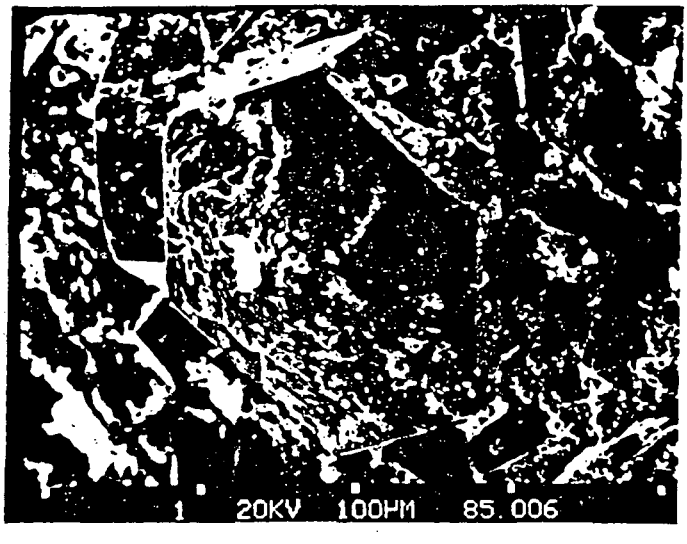

19

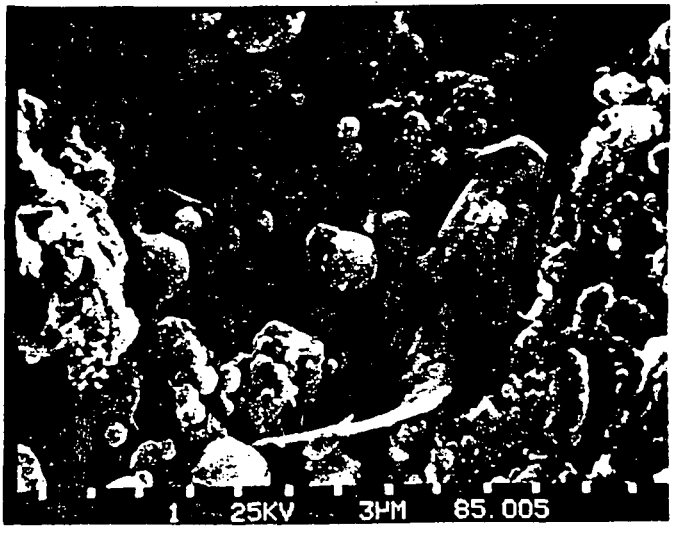

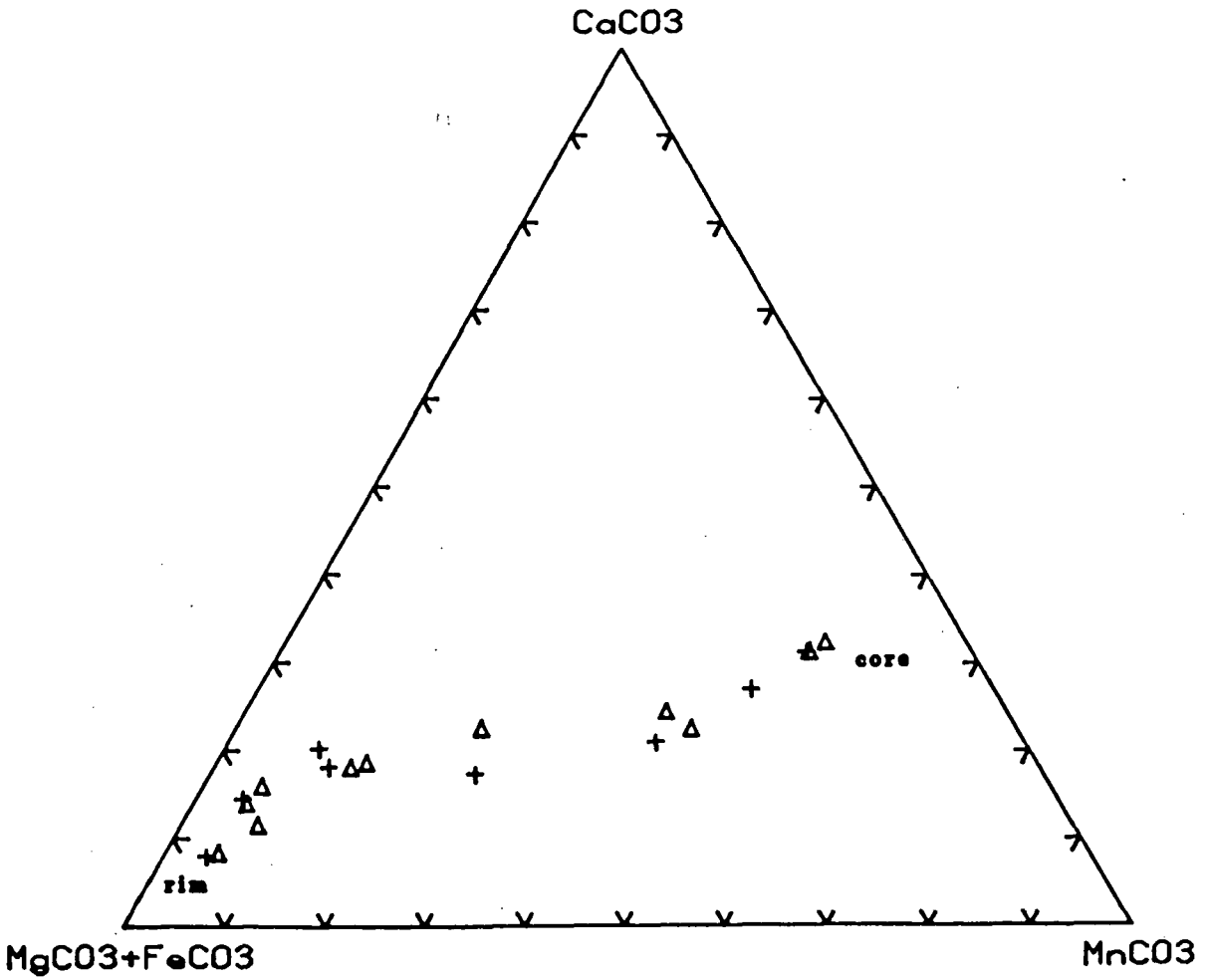
CaCO3
core
rim
MgCO3+FeCO3
MnCO3

20

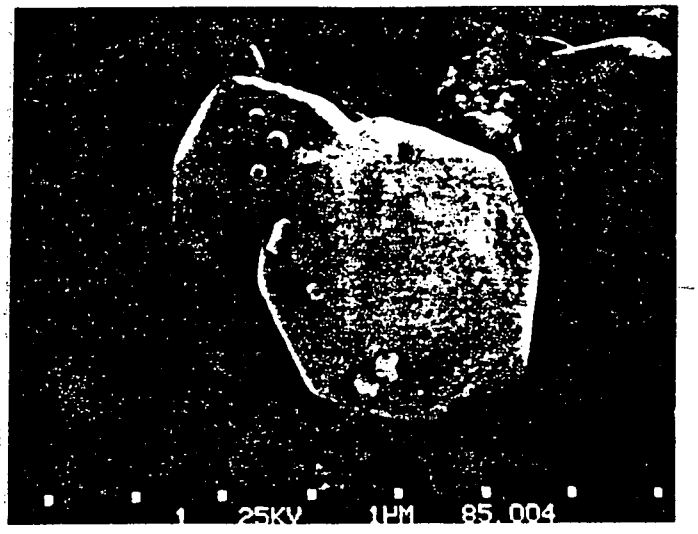

21

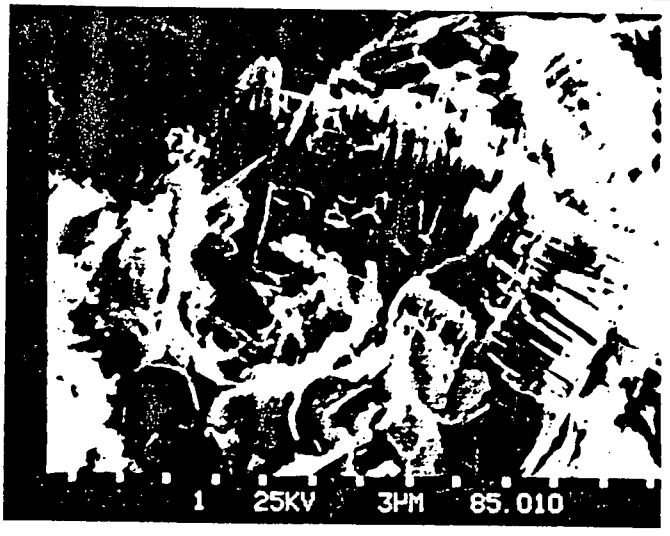

22

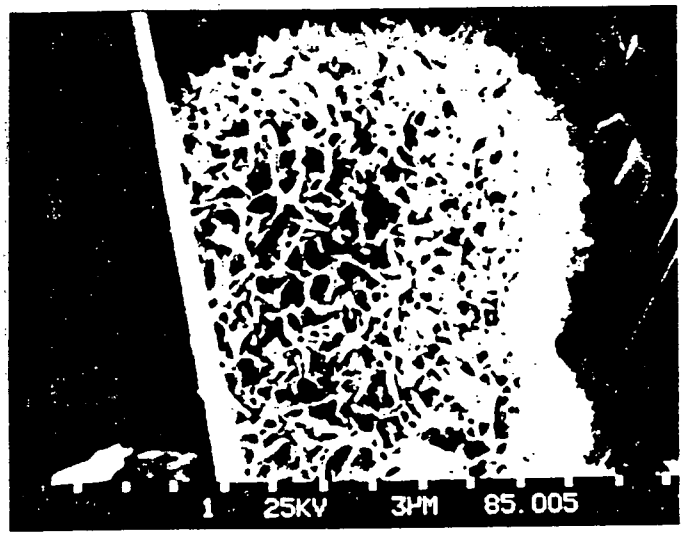

23

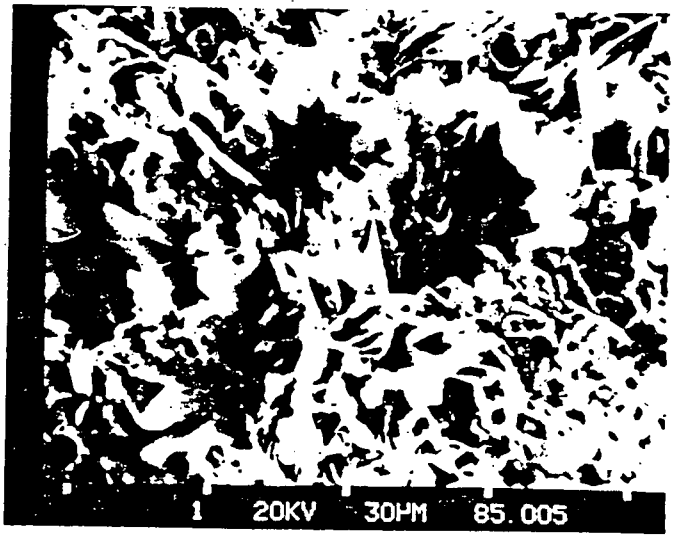

24

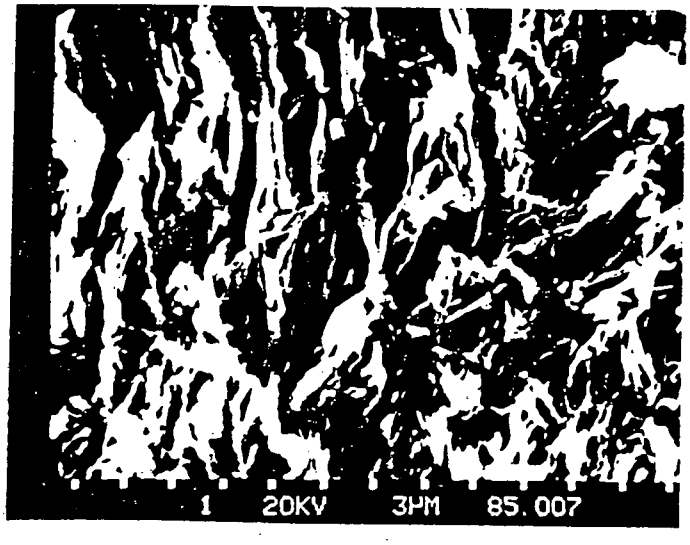

25

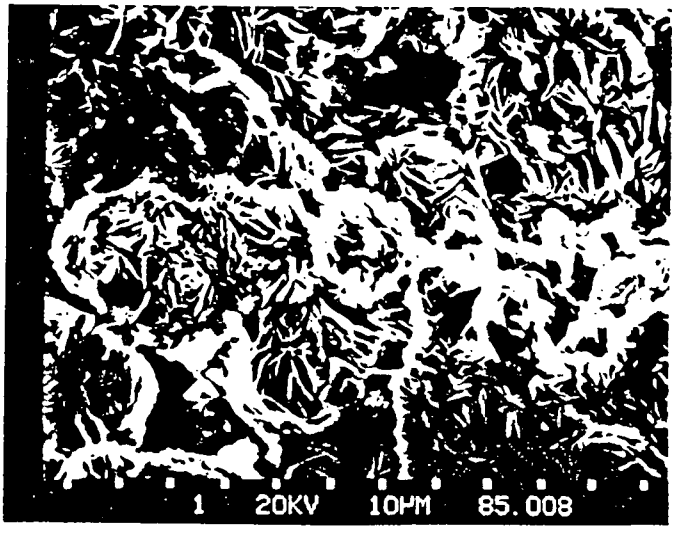

26

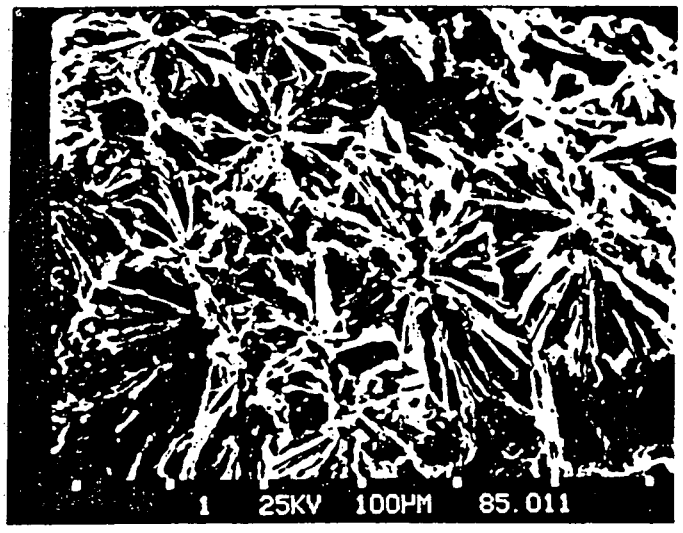

27

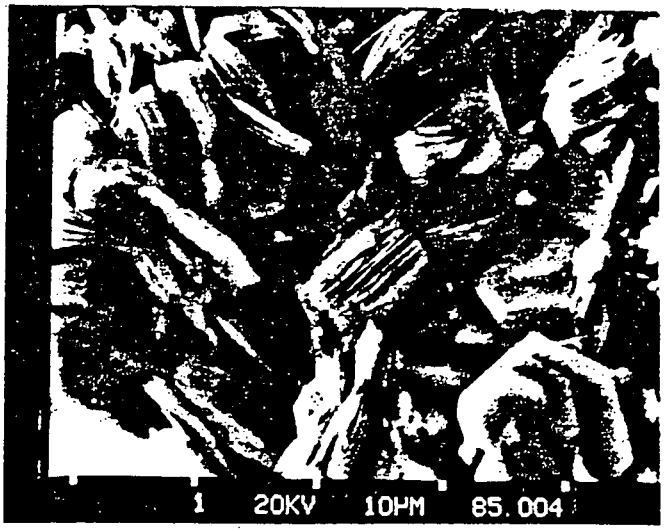

29

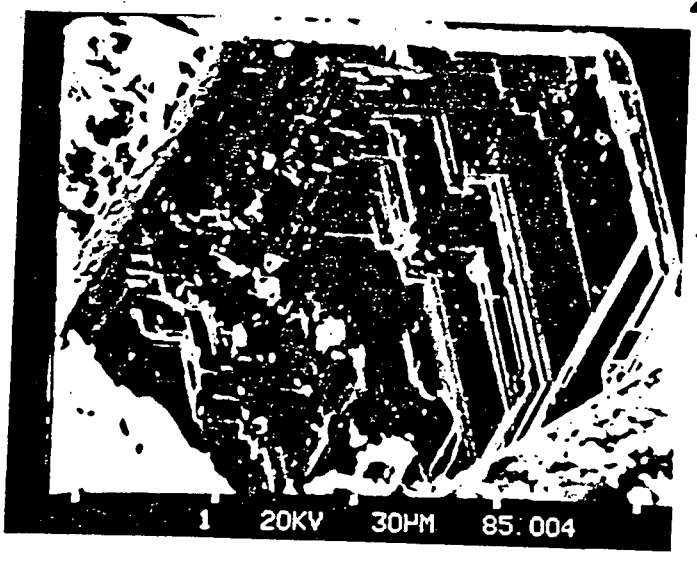

30

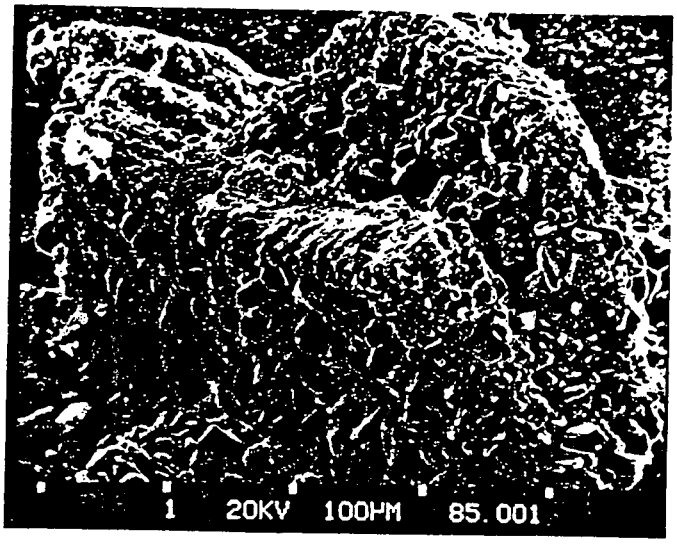

32

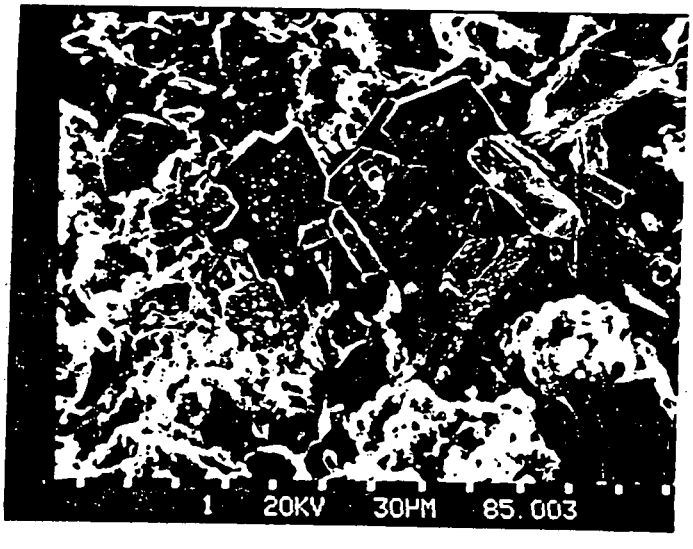

33A

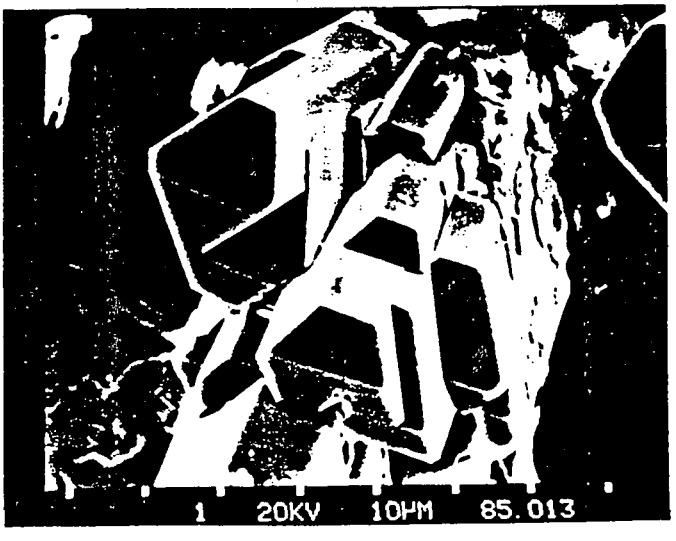

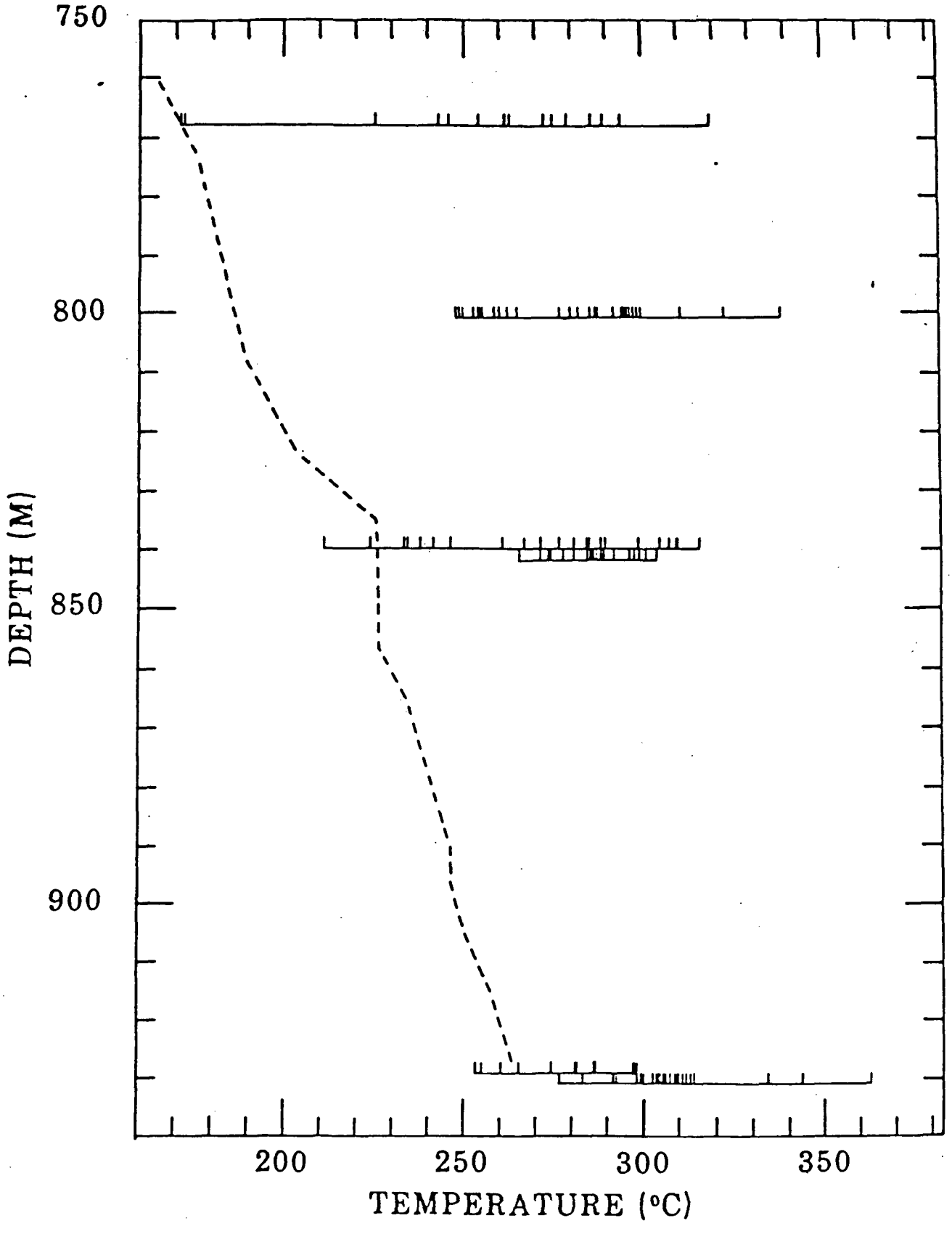
750
800
850
900
DEPTH (M)
200
250
300
350
TEMPERATURE (°C)

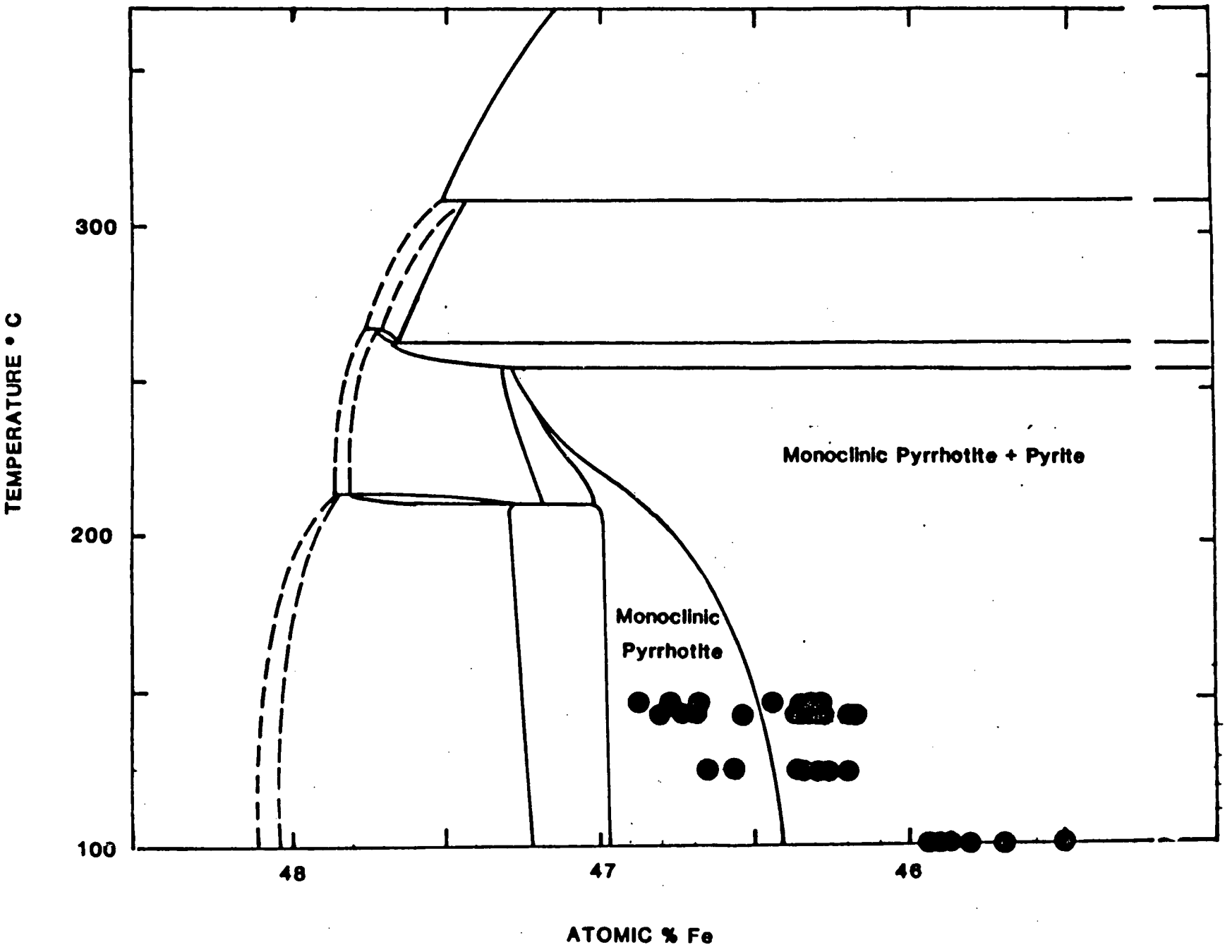
TEMPERATURE • C
300
200
100
48
47
46
ATOMIC % Fe
Monoclinic Pyrrhotite + Pyrite
Monoclinic
Pyrrhotite

34

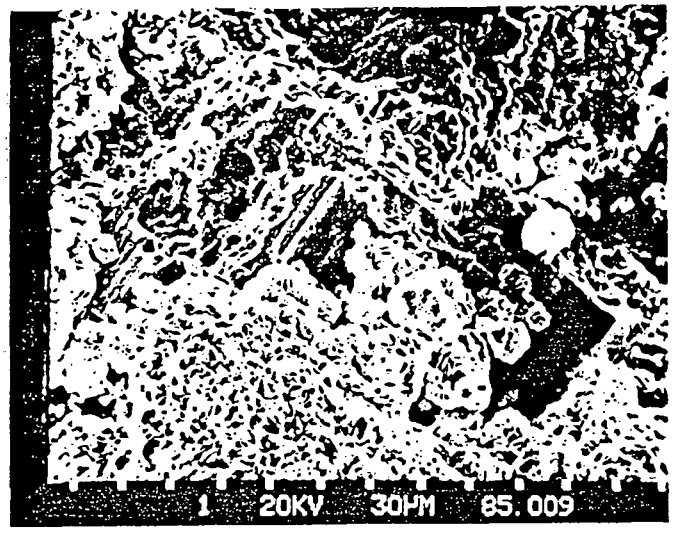

33B

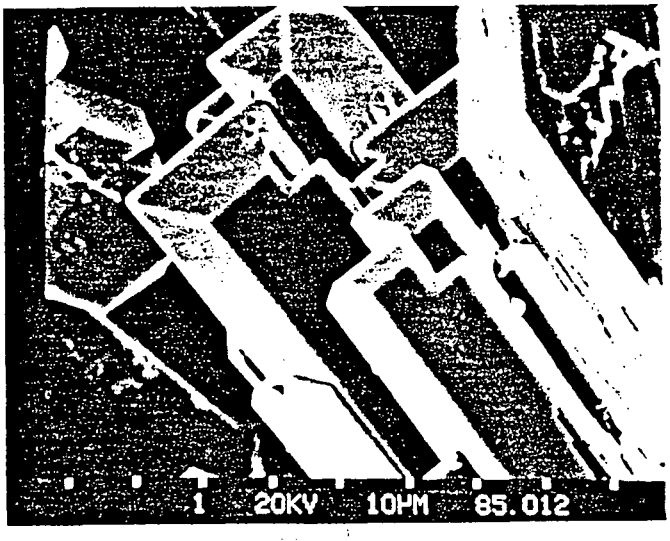

Newberry-2 265°C 932m

USGS says 740MWe for 30yrs (1979) (290)

Dobson 1116 MWe for 30yrs

- 40km SE Bend
- Large volcano 1300 km²
- Silicic and mafic
- Island arcuate Tumalo - Walker Rim Fz. Brothers Fz ± 20 mi north.
- summit caldera 6.4 x 8 km
- Caldera formation + eruptions began 320,000 yrs BP and have occurred sporadically until ± 30,000 yrs BP
- in caldera, felsic rocks younger than Mazama ash (6845 BP)
- Big obsidian flow 13.5 ka yr BP
- Mafic volcanoes 200,000 to 6,000 yrs old.
- vertical permeabilities are low in Newberry-2.
- 860 - 930 m Newberry-2 505°C/km

- no mag expression - pluton > 5 km pt?
- gravity anomaly indicates intrusion

- agreement that shallow pluton underlies caldera, but no agreement on boundaries of state.
  gravity 10 km dia, 2 km deep
  density contrast ±0.2 - 0.3 volcanics → batholith

- Blackwell says hot, molten intrusions under High Cascades @ 7 - 10 km depth -

- Silicic volc rocks 6200 - 13 000 years BP cover E part caldera
- rim of pluton - larger body is older - silicic eruptives over dia 18 km, but youngest is 3-4 km dia as most recent phase.

- temp in Bard averages 8.6°C = 47½°F
all volc rocks older than Mazama ash (6845 BP) are normal polarity - indicating younger than 700,000 yrs.

- East of Paulina lakes 2 km apart -- surface elev differ by 15 m.
- altered breccias are high permeability